Journal of Volcanology and Geothermal Research 419 (2021) 107363

Contents lists available at ScienceDirect

Journal of Volcanology and Geothermal Research

journal homepage: www.elsevier.com/locate/jvolgeores

Historical volcanism in the Canary Islands; part 1: A review of precursory and eruptive activity, eruption parameter estimates, and implications for hazard assessment

Marc-Antoine Longpré [a,b,*], Alicia Felpeto [c]

[a] School of Earth and Environmental Sciences, Queens College, City University of New York, Queens, New York 11367, USA
[b] Earth and Environmental Sciences, The Graduate Center, City University of New York, NY, New York 10016, USA
[c] Observatorio Geofísico Central, Instituto Geográfico Nacional, Madrid 28014, Spain

ARTICLE INFO

Article history:
Received 30 March 2021
Received in revised form 11 July 2021
Accepted 26 July 2021
Available online 28 July 2021

Keywords:
Canary Islands
Historical eruptions
Eruption chronology
Lava flow length
Eruptive volume
Volcanic hazards

ABSTRACT

Despite decadal–millennial repose periods, volcanoes of the Canary Islands pose significant, though poorly understood hazards to local communities and infrastructure. At least 13 volcanic eruptions forming monogenetic cones and lava flows have occurred in the archipelago since 1500 CE: six on the island of La Palma (in 1585, 1646, 1677–1678, 1712, 1949 and 1971), four on Tenerife (1704–1705, 1706, 1798 and 1909), two on Lanzarote (1730–1736 and 1824) and one on the submarine flank of El Hierro (2011–2012). In this paper, we synthesize available data on these historical eruptions, focusing on their physical characteristics and chronological development, and provide new estimates of eruption parameters, such as lava flow runout, area and volume, to inform volcanic hazard assessment in the archipelago. While incomplete and imprecise, historical records indicate that precursory seismicity began days to years prior to eruption onset, consistent with the three months of well-documented unrest for the 2011–2012 eruption. Excluding the atypical 1730–1736 event, eruptions lasted from ten days to a little under five months. Initial eruptive phases usually involved the opening of multiple vents along dike-fed fissures, with Strombolian explosive activity forming monogenetic cones. Lava flow emission generally quickly followed, and later eruptive phases were typically dominated by effusive behavior. Some eruptions (1704–1705, 1824 and 1949), however, had a complex evolution punctuated by the sequential opening of distinct vents several kilometers apart. Total lengths of vent-defined fissures range from 0.2 to 14.0 km, and maximum lava flow runout is 2.7–9.4 km, extending to the coastline in 75% of eruptions. Proximal eruptive deposits cover 1.8–7.8 km^2. Published estimates of subaerial eruptive volumes average between 11 and 66 $\times$ 10^6 m^3. In comparison, a new empirical relationship based on well-constrained lava flow area and volume data at other basaltic volcanoes yields volumes of 10–76 $\times$ 10^6 m^3 for Canary Island eruptions. The 1730–1736 Timanfaya eruption on Lanzarote represents an outlier in the context of historical Canary Island volcanism, with a duration of 2055 days, a total fissure length ≥ 14.4 km defined by at least ten main emission centers, a maximum lava flow length of 21.7 km, a lava flow field area of 146 km^2 and volume of at least 2.2–3.7 km^3. Historical eruptive rates are low, at 1.0–2.1 $\times$ 10^6 m^3/year or 7.3–11.0 $\times$ 10^6 m^3/year including the 1730–1736 eruption, in agreement with long-term volcano growth rates based on geologic data. We find no evidence for time-predictable or volume-predictable behavior of the historical eruptive sequence, which has a mean recurrence interval of 39 $\pm$ 24 years. Our analysis outlines a useful framework for forecasting the onset, development and style of future eruptions in the archipelago. Further work, particularly detailed field-based studies of eruption deposits and petrologic reconstructions of eruption run-up processes, will help refine our understanding of historical volcanism and associated hazards in the Canary Islands.

1. Introduction

Shield volcanoes building up ocean islands include the largest and some of the most active and best-monitored (e.g., Kīlauea, Piton de la Fournaise) volcanic edifices on Earth. Despite being dominated by effusive eruption styles, persistently active shield volcanoes pose significant hazards, the assessment of which may be complicated by the possibility of distal flank or rift zone eruptions combined with increasing island populations and infrastructures (Houghton et al., 2021; Michon et al., 2007; Neal et al., 2019). Quiescent shield volcanoes, in contrast, are dormant for decades to millennia between eruptions, which prevents quantification of precursory unrest and eruptive activity from the

* Corresponding author at: School of Earth and Environmental Sciences, Queens College, City University of New York, Queens, New York 11367, USA.
E-mail address: mlongpre@qc.cuny.edu (M.-A. Longpré).

https://doi.org/10.1016/j.jvolgeores.2021.107363
0377-0273/

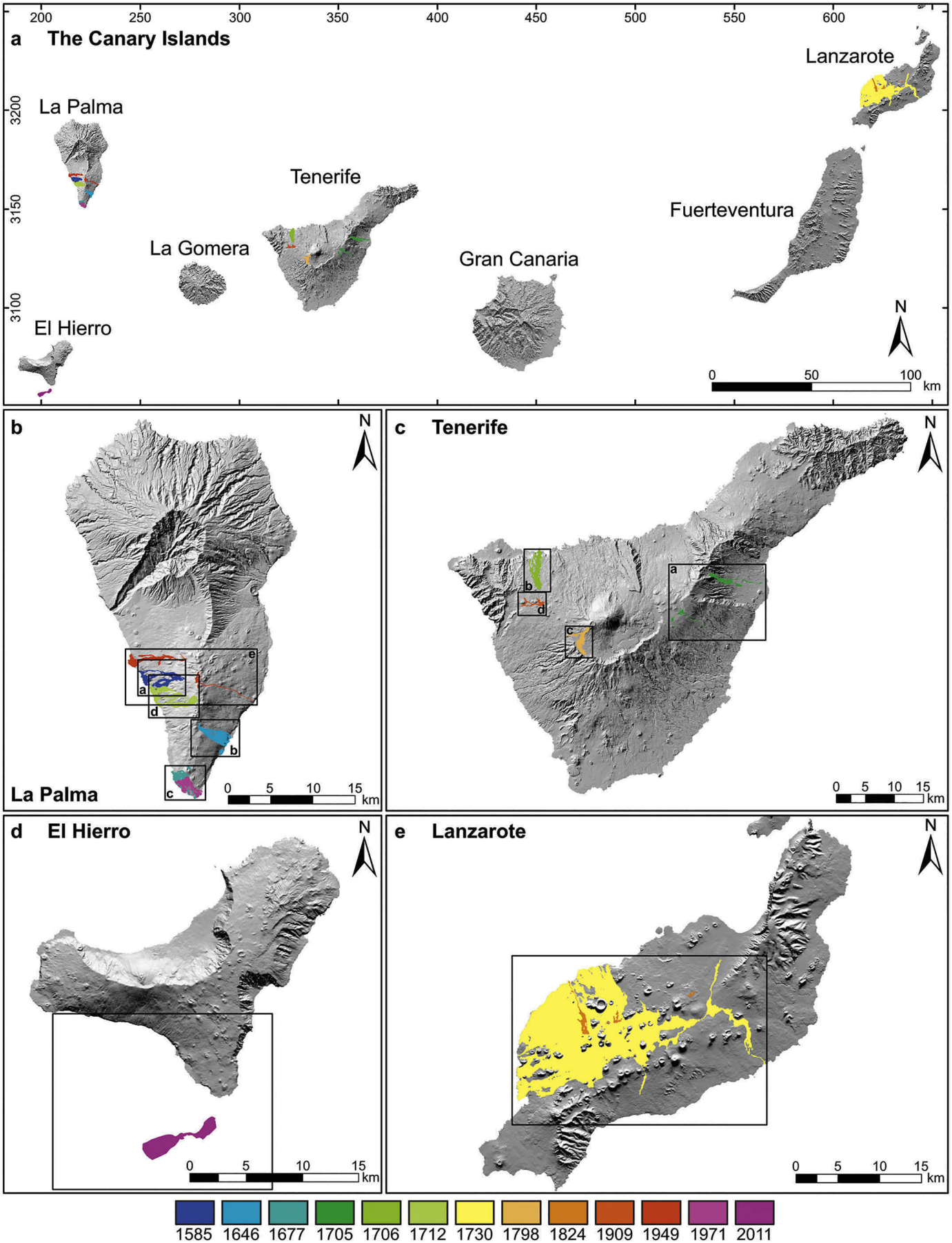

Fig. 1. Overview maps of (a) the Canary Archipelago, with UTM coordinates (zone 28 N; ellipsoid: WGS84; datum: REGCAN95) given in km, (b) La Palma, (c) Tenerife, (d) El Hierro and (e) Lanzarote showing the historical lava flow fields. Panels (b), (c), (d) and (e) show the areas enlarged in Figs. 2, 3, 5, and 4, respectively.

instrumental record and may lead local populations, authorities, and volcanologists to a biased perception of potential hazards (e.g., Gregg et al., 2004; Kueppers et al., 2019). Volcanoes of the Azores, Cape Verde, Galapagos, and Canary Islands, for example, can fall into this category.

The Canary Archipelago comprises seven main intraplate volcanic islands located in the eastern Atlantic Ocean and built on oceanic crust of Jurassic age (Fig. 1). Although still debated (e.g., van den Bogaard, 2013; Zaczek et al., 2015), their origin is thought to relate to a mantle plume impinging upon the slow-moving African Plate, as substantial geologic (Carracedo et al., 1998; Geldmacher et al., 2005), geochemical (Herzberg and Asimow, 2008; Hoernle and Schmincke, 1993), and geophysical (French and Romanowicz, 2015; Fullea et al., 2015) evidence suggests. The oldest radioisotopic ages of subaerial rocks display a broad (though discontinuous) progression from 20 Ma in the east (Fuerteventura) to 1.1 Ma in the west (El Hierro), yet all islands but La Gomera show evidence of Holocene volcanism (e.g., Paris et al., 2005).

In the historical period beginning in the 16th century, 13 confirmed volcanic eruptions have taken place in the Canary Islands: six on La Palma (in 1585, 1646, 1677–1678, 1712, 1949, and 1971), four on Tenerife (1704–1705, 1706, 1798, and 1909), two on Lanzarote (1730–1736 and 1824) and one on the submarine flank of El Hierro (2011–2012) (Figs. 1–5) (e.g., Carracedo et al., 2015; Romero Ruiz, 1990). All produced monogenetic cones of various forms and associated lava flow fields. Some of these events had profound impacts on the local population and infrastructure. Particularly, the 1706 Tenerife eruption partially destroyed the port town of Garachico (Solana and Aparicio, 1999) and the large 1730–1736 Timanfaya eruption on Lanzarote buried 26 villages along with vast agricultural land, transformed much of the island's landscape and forced exodus of the inhabitants (Carracedo et al., 1990, 1992; Romero, 2003). With a current and growing resident population of ~ 2.2 million (287 inhabitants per km^2) and ~ 17 million visitor entries per year (Instituto Canario de Estadística, 2016), the Canary Islands are increasingly susceptible to volcanic risk and future eruptions are likely to pose significant hazards to populations and impact infrastructure (Brown et al., 2015a)(). Patterns in precursory unrest and volcanic behavior for the historical period can help forecasting the onset, development and style of future eruptions (e.g., Bebbington and Jenkins, 2019; Sparks, 2003). However, only the 2011–2012 eruption was monitored with modern volcano surveillance techniques (López et al., 2012; Martí et al., 2013a) and, although previous works bearing on these aspects exist (Albert et al., 2016; Carracedo et al., 2001, 2015; Carracedo and Rodríguez Badiola, 1991; Romero Ruiz, 1990; Solana, 2012), a comprehensive synthesis of volcanological data on historical Canary Island eruptions is thus far lacking.

In this paper, we gather available data on historical eruptions in the Canary Islands to inform volcanic hazard assessment in the archipelago. A companion article (Longpré et al., in prep.) presents new data on tephra compositions for the same eruptions and discusses petrogenetic implications. After a brief summary of previous work, we provide summaries of the 13 historical eruptions, focusing on their main physical characteristics and chronological development. An analysis of available eruption parameters, including lava flow length, area and volume, is then presented, followed by a discussion of eruptive rates and long-term eruption forecasting. A final section outlines some implications for regional volcanic hazards.

2. Previous work

Most previous studies providing relevant data pertaining to historical eruptions in the Canary Islands have narrowed in on a single event and their important contributions are summarized in Section 3. Among the first modern works presenting broader overviews, Hernandez-Pacheco and Valls (1982) focused on a structural and petrologic analysis of La Palma eruptions but also compiled a list of confirmed and possible historical eruptions across the archipelago. The subsequent work of Romero Ruiz (1990) is particularly important as it presented an exhaustive analysis of most available eyewitness accounts, which were transcribed in an appendix. While focusing on the 1730–1736 eruption, Carracedo and Rodríguez Badiola (1991) substantiated the compilation of Hernandez-Pacheco and Valls (1982) by adding estimates of planimetric areas affected by all historical eruptions. Carracedo et al. (2001) provided updated summaries of all La Palma eruptions. To quantify long-term probabilities of future eruptions, Sobradelo et al. (2011) approximated dense rock equivalent volumes for both lava and proximal tephra for all eruptions based on analysis of geologic maps and digital elevation models. Concentrating on Tenerife eruptions, Solana (2012) reviewed the historical documents assembled by Romero Ruiz (1990) and presented new field- and map-based data (e.g., lava flow length, area and volume) to reconstruct the development of lava flow fields. Carracedo (2013) discussed the last 2 ky of volcanism on Tenerife and synthesized the chronology and physical features of the island's historical eruptions supported by geologic maps, while Carracedo et al. (2013) added lava flow length, area and volume estimates and addressed volcanic hazards. Carracedo et al. (2015) primarily reviewed data relating to the 2011–2012 El Hierro eruption, but also presented an updated table with new and revised values for area and volume estimates of other historical eruptions. In a field-guide perspective, Carracedo and Troll (2016) summarized the main features of all historical eruptions and accompanied their descriptions by rich illustrations. Finally, Sánchez (2014), Albert et al. (2016) and Rueda Núñez et al. (2020) recently systematically reanalyzed the historical accounts to extract records of felt seismicity precursory to and accompanying eruptions.

3. Historical eruptions in the Canary Islands

Here we present summaries of historical Canary Island eruptions for those events with confirmed dates and locations. We therefore do not discuss the 15th century eruption at Tacande/Montaña Quemada, La Palma, whose timing is uncertain (Carracedo et al., 2001), and that of 1492 observed by Christopher Columbus, which was assigned to Boca Cangrejo volcano on Tenerife based on radiocarbon dating (Carracedo et al., 2007). A questionable submarine event at El Hierro in 1793 is also excluded (Carracedo et al., 2015; Villasante-Marcos and Pavón-Carrasco, 2014). For each event, we divide our analysis in terms of (1) the main physical characteristics of the eruptions and (2) the chronology and nature of precursory and eruptive phenomena. Erupted magma composition is briefly mentioned (see companion paper for details). Our synthesis relies largely on published data, which are compiled in Tables 1 and A.1–A.2. New data on eruption parameters presented in Table 2 were acquired via geographic information system (GIS) analysis of open-source orthophotos, digital elevation models (DEM) (both from the Instituto Geográfico Nacional, IGN, www.ign.es) and geologic maps (from the Instituto Geológico y Minero de España, IGME, www.igme.es) using ArcGIS and Google Earth software. New eruptive volume estimates quoted in the text are derived from Eq. 2 (see Section 4.5).

Reconstructions of eruption chronologies presented in Fig. 6 and Tables A.3–A.13 are mostly based on the work of Romero Ruiz (1990) and a reanalysis of the eyewitness accounts collated therein. Data from other sources are also integrated where available. Records of pre-eruptive and *syn*-eruptive felt seismicity are from Sánchez (2014) (see Rueda Núñez et al., 2020). Due to their specificity, the chronologies of the 1730–1736 and 2011–2012 eruptions are presented separately in Figs. 7–8 and Tables A.14–A.15. At the outset, it must be emphasized that historical records are largely incomplete and imprecise, and thus only partial eruption reconstructions are possible. In addition, the early phases of eruptions tend to be much better documented than later phases. In this context, our approach consisted in compiling confirmed occurrences of specific phenomena for which specific dates are given. These phenomena include (1) *felt seismicity*, (2) *the opening of a new vent or fissure*, (3) *explosive activity*, (4) *lava effusion* and (5) *the*

Table 1
Published chronological and volcanological data on historical Canary Island eruptions.

Year	I[a]	*Eruption*/Volcano[b]		P[c]	O[d]	E[e]	D[f]	r_1[g]	r_2[h]	A[i]	V[j]	H[k]	C[l]
1585	LP	Jedey/Tajuya		~50	19-May	10-Aug	84	93	93–155?	3.7	24 (7)	–	BN, P, T
1646	LP	Tigalate/Martín		1	1-Oct	21-Dec	82	61	61	7.0	26 (5)	–	BN
1677–78	LP	*Fuencaliente*		4	17-Nov	21-Jan	66	31	31	4.5	66 (43)	–	BN
1704–05	TF	Siete Fuentes		7	31-Dec-04	5-Jan-05	6–17[m]	27	≥212	5.2 (1.8)	37 (22)	–	BN
		Fasnia			5-Jan	15-Jan	11–21[p]					–	BN
		Arafo			2-Feb	27-Mar	54					≥1	BN
1706	TF	*Garachico*/Negra		404	5-May	~13-Jun	9–40[m]	1	1	7.9 (2.0)	54 (8)	1.5	BN, T
1712	LP	El Charco/Lajiones		5	9-Oct	3-Dec	56	6	35	10.2	41 (30)	–	BN, T
1730–36	LZ	*Timanfaya*	Cuervos	~1500?	1-Sep-30	19-Sep-30	2055	18	≥14,500?[n]	187 (33)	2482 (1433)	–	BN
			Santa Catalina		10-Oct-30	31-Oct-30							BN, B
			Pico Partido		10-Oct-30	Jan-31							BN, B
			Señalo		Mar-31	Jun-31							B
			El Quemado		Jun?-31	Jun?-31							B
			Rajada		Jul?-31	Jul?-31							B
			Quemadas		Dec?-31	Jan?-32							B
			Fuego		1732?	1736?							B
			Nueces		Feb?-33[o]	Apr?-36							B
			Colorada		2?-Apr-36	16-Apr-36							B
1798	TF	Chahorra		1090	9-Jun	15-Sep	92[p]–98+[m]	68	92	4.5 (0.5)	30 (13)	≥1	PT
1824	LZ	Tao		2, ~4000?	31-Jul	1-Aug	86	26	94	5.0	11 (11)	–	BN
		Nuevo del Fuego			29-Sep	5-Oct							
		Tinguatón			16-Oct	24-Oct							
1909	TF	Chinyero		605	18-Nov	27-Nov	9[p]–10	85	111	2.0 (0.6)	15 (8)	1	BN, T
1949	LP	*San Juan*	Duraznero	884	24-Jun	30-Jul	37[q]	40	237	4.8	51 (51)	1.5	BN, T
			Llano del Banco		8-Jul	26-Jul						0.03	BN, T
			Hoyo Negro		12-Jul	30-Jul						0.7	BN, PT
1971	LP	Teneguía		6	26-Oct	18-Nov	24	22	22	3.7 (0.8)	31 (13)	0.2	BN, T
2011–12	EH	Tagoro (submarine)		96[r]	10-Oct[r]	15-Feb[s]	128[s]	40	≥218	5.0	329	n.a.	BN

– = no data; n.a. = not applicable
[a] I=Island: EH = El Hierro; LP = La Palma; LZ = Lanzarote; TF = Tenerife.
[b] Eruption names are in italic. Volcano names are abbreviated (e.g., the words "Volcán (de)", "Montaña (de)" or "Caldera (de)" are omitted), see text.
[c] P=Duration of precursory felt seismicity in days before eruption onset. From Sánchez (2014) unless otherwise noted.
[d] O=Date of eruption onset. Data for 1730–1736 from Carracedo et al. (1992); the remainder are from Romero Ruiz (1990) unless otherwise noted.
[e] E = Date of eruption end. Data for 1730–1736 from Carracedo et al. (1992); the remainder are from Romero Ruiz (1990) unless otherwise noted.
[f] D = Eruption duration in days. From Romero Ruiz (1990) unless otherwise noted.
[g] r_1 = Repose period in years since onset of previous Canary Island eruption.
[h] r_2 = Repose period in years since onset of previous eruption on the same island.
[i] A = Planimetric area of proximal eruption deposits. Mean published value, with standard deviation in parentheses, in km^2. Details in Table A.14.
[j] V=Bulk volume of proximal eruption deposits. Mean published value, with standard deviation in parentheses, in millions of m^3. Details in Table A.15.
[k] H = Maximum reported eruption column height, in km. See text for details.
[l] C=Composition of erupted products: B = basalt; BN = basanite; T = tephrite; PT = phonotephrite; P = phonolite.
[m] Solana (2012)
[n] Carracedo et al. (2003)
[o] Pallarés Padilla (2007), Carracedo (2014)
[p] Carracedo et al. (2013)
[q] Klügel et al. (1999)
[r] López et al. (2012)
[s] Sánchez-Pastor et al. (2018)

arrival of lava at the coast, of which only the first instance is compiled. Occurrences are "rounded" on a daily basis, i.e., whether one or one hundred felt earthquakes were reported for a given day, only one star symbol appears for that day on Fig. 6. The category "*explosive activity*" refers to any type of pyroclastic activity because eruption style typically cannot be confidently inferred from the historical records. However, observations of 20th century eruptions and the general character of tephra deposits suggest that explosive phases of historical eruptions were dominated by Strombolian activity (e.g., Araña and Fuster, 1974; Carracedo and Troll, 2016), although violent Strombolian (Di Roberto et al., 2016) and phreatomagmatic activity (White and Schmincke, 1999) also occurred. The specific categories "*lava dome*", "*hydrothermal activity*", and "*phreatomagmatic activity*" can be confidently applied to the 1585, 1824, and 1949 eruptions, respectively. Finally, we assigned the categories "*unspecified seismicity*" and "*unspecified eruptive activity*" to the common cases for which seismicity and eruptive activity can be inferred to have taken place *within* a period of time but cannot be ascribed to specific days and/or styles (for eruptive activity, whether explosive and/or effusive). Such unspecified activity needs not have been continuous.

3.1. The 1585 Jedey eruption, La Palma

The Jedey eruption on La Palma occurred in the northern part of the western flank of Cumbre Vieja volcano at an altitude of ~ 1015 m (Fig. 2a). Several cinder cones (Volcán de Jedey or de Tajuya) were constructed, reaching a maximum height of 95 m, and define a ~ 1.5-km-long eruptive fissure. A lava flow field comprising three main branches, the southernmost of which was partially covered by the 1712 flows, reached up to 4.6 km from source, forming coastal platforms upon entering the sea. Previous works report a proximal deposit area of 3.7 km^2 and a volume of 24 ± 7 (1σ) $\times 10^6$ m^3 (Tables 1, A.1–A.2). In comparison, we obtain a proximal deposit area of 4.5 km^2 and a volume of 36×10^6 m^3 (Table 2). In addition to producing basanite–tephrite pyroclasts and lavas, this eruption was also characterized by the extrusion of phonolite lava domes/spines, named the Roques de Jedey. Interestingly, the origin of these phonolite domes — either accidental prehistoric units uplifted by the erupting mafic magma, part prehistoric and part juvenile, or entirely juvenile — is unclear (Carracedo and Troll, 2016), but they appear to have been highly viscous to solid upon emplacement.

Table 2
Physical characteristics and eruption parameter estimates for historical Canary Island eruptions.

Year	I[a]	*Eruption*/Volcano[b]		Z_V[c]	$Z_{L\ min}$[d]	F[e]	H_V[f]	L_1[g]	L_2[h]	θ_1[i]	θ_2[j]	A_L[k]	A_T[l]	V_1[m]	V_2[n]
1585	LP	Jedey/Tajuya		1015	0	1.5	95	4.60	4.49	12.4	12.8	3.78	4.51	79	36
1646	LP	Tigalate/Martín		1340	0	4.2	60, 200	4.13	4.30	18.0	17.3	4.44	4.50	79	36
1677–78	LP	*Fuencaliente*		450	0	0.9	15	3.46	3.30	14.3	7.8	2.29[o]	2.43[o]	79[p]	36[p]
1704–05	TF	Siete Fuentes		2240	1735	10.4	30	2.64	2.47	10.8	11.6	0.19	0.24	81	37
		Fasnia		2180	905		45	6.36	5.92	11.3	12.2	0.68	0.85		
		Arafo		1490	44		100	9.40	9.30	8.7	8.8	3.29	3.53		
1706	TF	*Garachico*/Negra		1345	0	0.9	105	6.69	6.55	11.4	11.6	7.45	7.78	136	76
1712	LP	El Charco/Lajiones		1625	0	2.5	95	5.11	4.49	17.6	19.9	3.78	4.51	79	36
1730–36	LZ	*Timanfaya*	Cuervos	320	0	14.4	65	21.68	15.74	1.0	1.3	146	148	2585	4330
			Santa Catalina	355			55								
			Pico Partido	390			110								
			Señalo	365			95								
			El Quemado	60			15								
			Rajada	255			120								
			Quemadas	320			45								
			Fuego	415			95								
			Nueces	360			40								
			Colorada	365			100								
1798	TF	Chahorra		2660	2015	1.0	45	5.36	4.25	6.9	8.6	4.01	4.60	80	37
1824	LZ	Tao		295	260	14.0	20	0.40	0.35	5.0	5.8	0.16	0.28	49	19
		Nuevo del Fuego		330	0		50	6.34	6.62	3.0	2.8	1.76	1.90		
		Tinguatón		310	275		25	1.35	1.30	1.5	1.5	0.51	0.62		
1909	TF	Chinyero		1505	1035	0.5	50	4.50	4.09	6.0	6.6	1.71	1.81	32	10
1949	LP	*San Juan*	Duraznero	1810	115	3.3	85	7.11	6.71	13.4	14.2	0.46	0.62	68	29
			Llano del Banco	1185	0		0	6.99	6.71	9.6	10.0	3.24	3.26		
			Hoyo Negro	1880	n.a.		20	n.a.	n.a.	n.a.	n.a.	n.a.	n.a.		
1971	LP	Teneguía		360	0	0.2	130	2.72	2.39	7.6	8.6	2.57	3.02	53	21
2011–12	EH	Tagoro (submarine)		−88	−1863	0.5	235	7.02	6.67	14.2	14.9	–	6.94	n.a.	n.a.

[a] I=Island: EH = El Hierro; LP = La Palma; LZ = Lanzarote; TF = Tenerife.
[b] Eruption names are in italic. Volcano names are abbreviated (e.g., the words "Volcán (de)", "Montaña (de)" or "Caldera (de)" are omitted), see text.
[c] Z_v = Altitude of main vent crater in m above sea level.
[d] $Z_{L\ min}$ = Minimum altitude of lava flow toe in m above sea level.
[e] F = Length of vent-defined eruptive fissure in km. Fissures may be discontinuous, see text.
[f] H_v = Maximum height of volcano/vent in m, measured as per the method of Kervyn et al. (2012). Data for 1730–1736 from Kervyn et al. (2012).
[g] L_1 = Maximum length of lava flow along main flow path in km.
[h] L_2 = Maximum length of lava flow taken in a straight line in km.
[i] θ_1 = Ground slope angle (in degrees) between crater and lava toe using L_1.
[j] θ_2 = Ground slope angle (in degrees) between crater and lava toe using L_2.
[k] A_L = Planimetric area of lava flow field in km^2.
[l] A_T = Planimetric area of lava flow field and proximal pyroclastic deposits in km^2.
[m] V_1 = Eruptive volume (in millions of m^3) calculated with Eq. 1 with A_T values as input. Eq. 1 likely overestimates volumes for small eruptions.
[n] V_2 = Eruptive volume (in millions of m^3) calculated with Eq. 2 with A_T values as input.
[o] Underestimate because deposits were partly covered by 1971 eruption. Use value of 4.5 km^2 (Carracedo et al., 1996, 2015) (Tables 1, A14).
[p] Calculation uses A_T = 4.5 km^2, see preceding footnote. n.a. = not applicable.

Based on eyewitness accounts summarized by Romero Ruiz (1990), the eruption lasted 84 days from 19 May to 10 August 1585 (Fig. 6a, Tables 1, A.3). Precursory felt seismicity occurred in the months immediately preceding eruption, but its onset is not precisely reported. Extrusion of the phonolite lava domes seems to have begun at the eruption's inception, accompanied by ground cracking and significant seismicity. The domes continuously collapsed, probably yielding small pyroclastic flows. New eruptive fissures opened up on the night of 26 May, in the upper part of the vent area. Gradual extrusion of the lava domes accompanied by Strombolian activity is inferred to have continued until the end of June. At this time, both seismic and volcanic activity increased in intensity. Various points of emissions produced explosions that dispersed fine pyroclastic material to significant, though unspecified, distance, and lava flows were also emplaced. Subsequently, the activity gradually decreased and entered a lull before explosive activity resumed in a final eruptive phase of unknown duration.

3.2. The 1646 Tigalate eruption, La Palma

The Tigalate or Martín eruption on La Palma occurred in the central part of Cumbre Vieja volcano, on its eastern flank (Fig. 2b). This eruption involved two main vents: an upper one at an elevation of ~ 1340 m above sea level and a lower one near the coast. Note that it is unclear whether Volcán Martín, a large, ~ 200-m-high cinder cone, was formed during this event, or the 1646 activity was sourced from smaller vents on the south flank of the Martín cone (Carracedo and Troll, 2016). Carracedo et al. (2001) reported arguments that suggest a prehistoric age for the Martín cone; hence, we suggest using the name Volcán de Tigalate to refer to this event to avoid possible confusion. Assuming Martín is indeed prehistoric and the lower vent is part of the eruptive fissure, a fissure length of 4.2 km is obtained (5.1 km if the Martín cone is included). Two distinct lava flow fields formed, one associated with each vent clusters, and reached a maximum distance from source of 4.1 km at the shoreline, producing coastal platforms. According to our estimate, the proximal deposits of the eruption cover 4.5 km^2. An area of 7 km^2 reported by Carracedo et al. (2015) may include the Martín lava flow. The mean published volume estimate is $26 \pm 5 \times 10^6$ m^3 (Tables 1, A.2), while we report a value of 36×10^6 m^3 (Table 2). The composition of eruptive products is basanite.

This eruption lasted 82 days, from 1 or 2 October to 21 December 1646, but historical accounts of it are scarce (Romero Ruiz, 1990) (Fig. 6b, Tables 1, A.4). The first reported sign of unrest consisted of felt seismicity occurring on 30 September, only 1–2 days before eruption. Ground cracks, gas emissions and a dense eruption column marked the onset of volcanic activity on 1 October. Seismic activity intensified from 1 to 4 October. New vents opened on 2 October, and again from 4 to 8 October, with a total of 9 reported vents. Early activity appears to have been dominantly explosive, with effusive behavior starting on

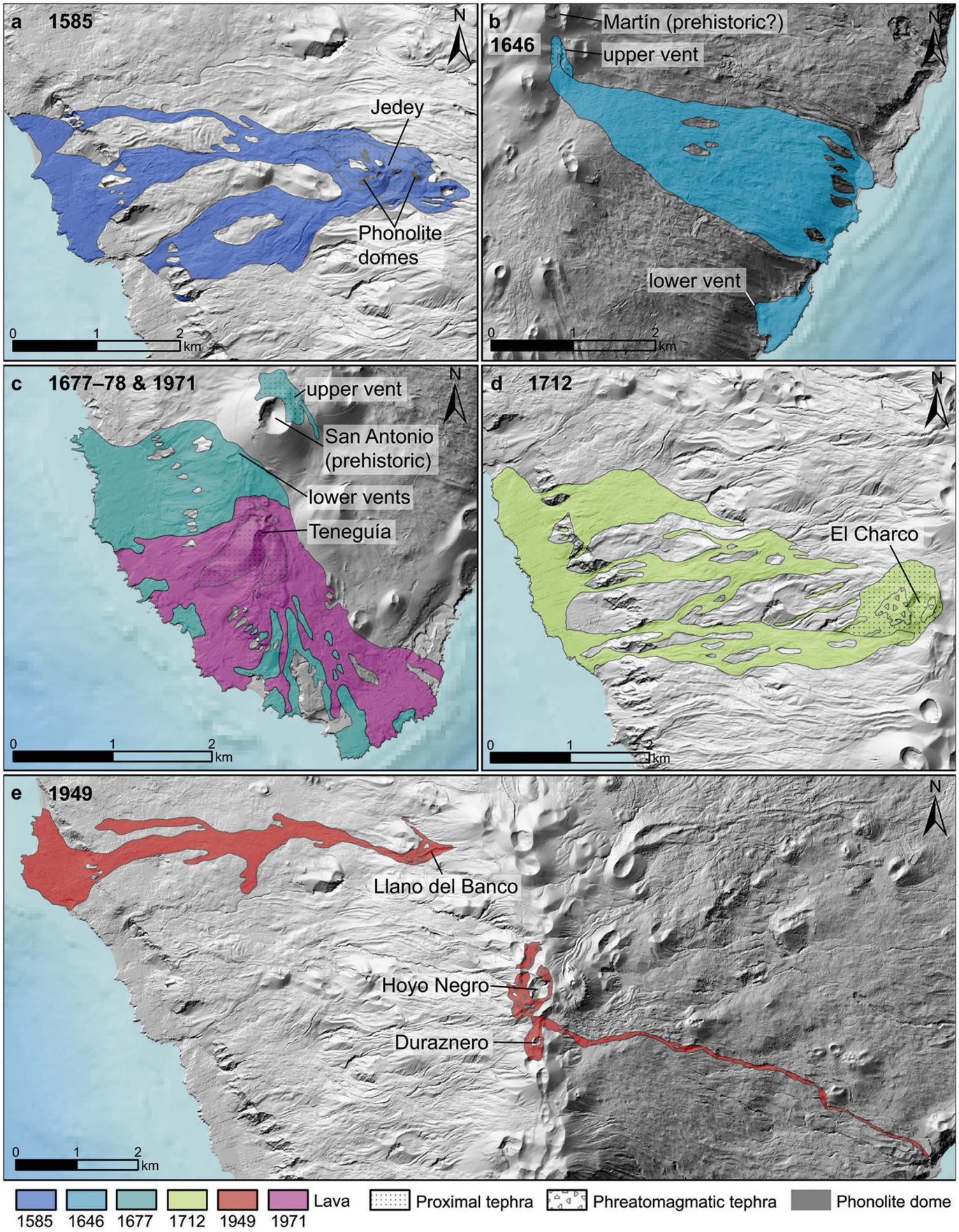

Fig. 2. Maps of historical eruption deposits on La Palma, modified after IGME: (a) the 1585 eruption (note the occurrence of phonolite domes in the vent area); (b) the 1646 eruption; (c) the 1677–1678 and 1971 eruptions; (d) the 1712 eruption; and (e) the 1949 eruption.

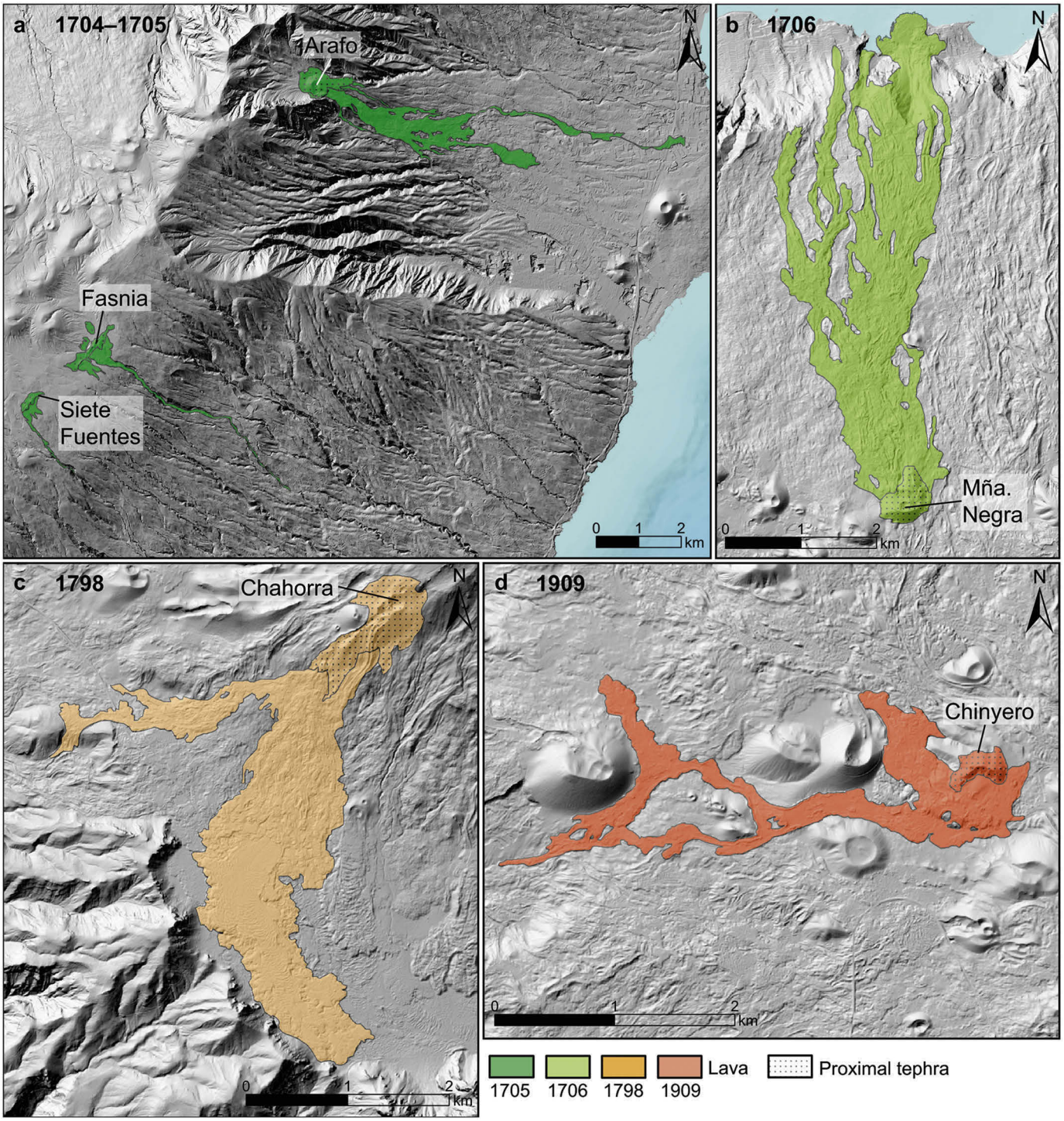

Fig. 3. Maps of historical eruption deposits on Tenerife, modified after IGME: (a) the 1704–1705 eruption; (b) the 1706 eruption; (c) the 1798 eruption; and (d) the 1909 eruption.

4 October. This first phase of activity took place at high elevation, at the upper vent. No other records are available until 15 November, when seismic activity accompanied the opening of a new fissure at low elevation near the coast, marking a second, dominantly effusive eruptive phase.

3.3. The 1677–1678 Fuencaliente eruption, La Palma

This eruption occurred near the town of Fuencaliente towards the southern tip of Cumbre Vieja volcano at ~ 450 m of altitude (Fig. 2c). Carracedo et al. (1996) presented a detailed reconstruction of this eruption based on geologic data and a review of historical documents. This analysis showed that, previously misassigned to the large phreatomagmatic Volcán de San Antonio, the 1677–1678 eruption had in fact originated from a small vent (15-m high), perched on the northeast rim of the San Antonio cone, as well as from spatter vents, located at its southwestern base, defining a 0.9-km-long fissure. As the 1971 eruption covered part of the 1677–1678 lavas, Carracedo et al. (1996) utilized pre-1971 aerial photos to assess the original extent of the 1677–1678 lava flow field. Four main flows with a maximum runout of 3.5 km all reached the coast and covered at least 4.5 km^2. Based on estimated lava thicknesses (10–15 m on the slopes, 30–50 m on coastal

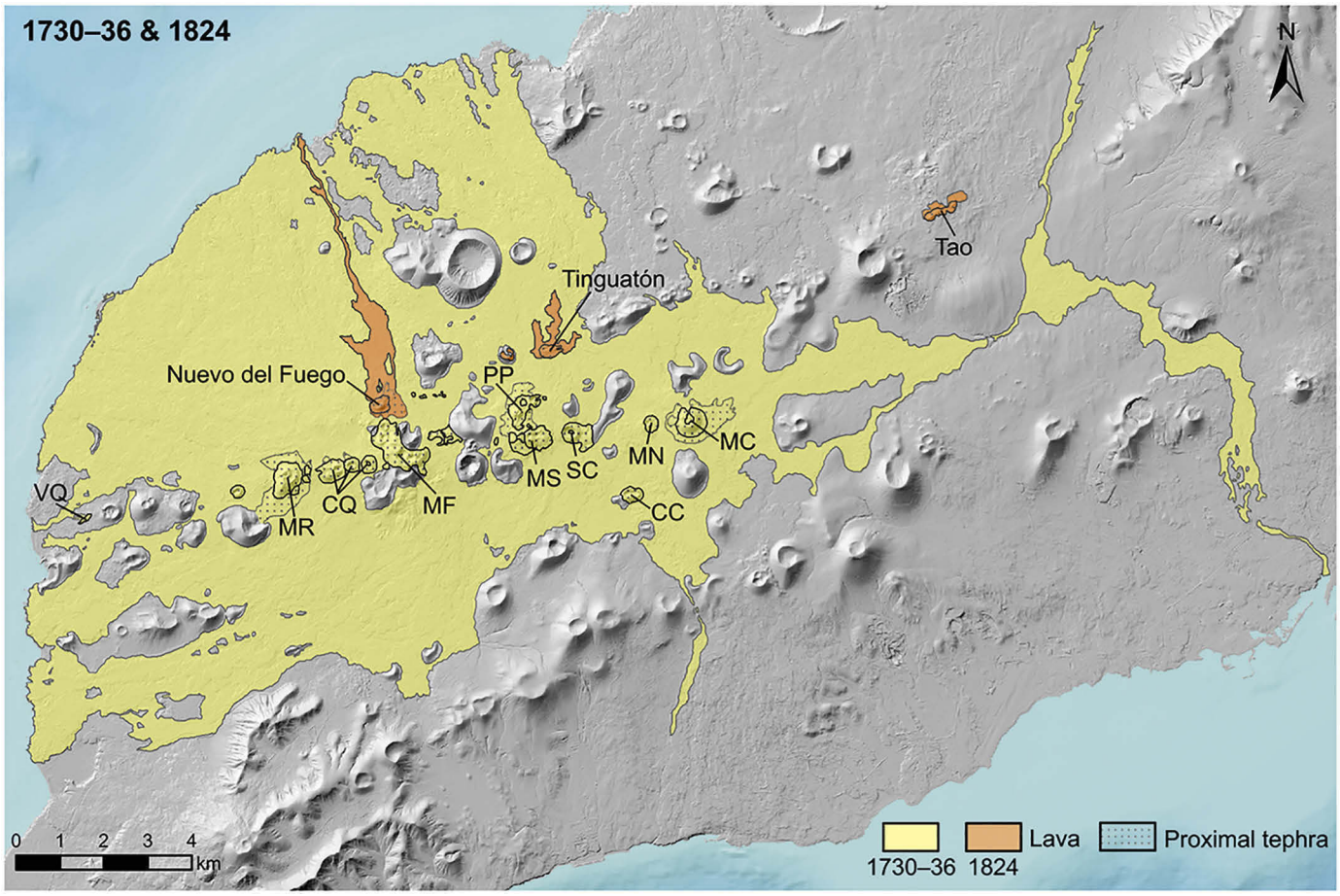

Fig. 4. Map of historical eruption deposits on Lanzarote, modified after IGME and Carracedo and Rodríguez Badiola (1991). For the 1730–1736 Timanfaya eruption, the lava flow field and pyroclastic deposits proximal to the cinder cones are shown (medial to distal tephra is omitted). Cinder cone names are abbreviated: CC: Caldera de los Cuervos; PP: Pico Partido; SC: Caldera de Santa Catalina; MS: Montañas del Señalo; VQ: Volcán El Quemado; MR: Montaña Rajada; CQ: Calderas Quemadas; MF: Montañas del Fuego; MN: Montaña de las Nueces; MC: Montaña Colorada.

platforms), an estimated lava volume of 76–122 $\times$ 10^6 m^3 is obtained (Carracedo et al., 1996). The mean published value is 66 $\pm$ 43 $\times$ 10^6 m^3, while we obtain 36 $\times$ 10^6 m^3 (Tables 1–2, A.1–A.2). Eruptive products show a basanitic composition.

The Fuencaliente eruption lasted 66 days from 17 November 1677 to 21 January 1678. Our summary of the chronological development of the events is based on Carracedo et al. (1996) and integrates additional details reported by the historical sources (Romero Ruiz, 1990) (Fig. 6c, Tables 1, A.5). Felt precursory seismicity began on 13 November 1677, only four days before eruption onset. During a first eruptive phase, on 17 November, fractures opened up on the northeast flank of the pre-existing San Antonio cone, emitting steam and sulfuric gases. At 4:30 pm, a fissure opened at the southwestern base of the San Antonio cone, producing spatter and fluid lavas that flowed towards the south then southwest and reached the coast. On 19 November, marking the onset of a second eruptive phase, new vents opened extending the lower fissure to the northwest, which emitted lava flowing towards the southwest that formed a wide coastal platform. Steam emissions from the upper fracture northeast of the San Antonio cone were reported to increase on 20 November, and explosive activity at this locality apparently began on 21 November. Historical accounts report pyroclastic material to have reached the sea. Three notably powerful explosions were reported on 23 November. A third eruptive phase began on 26 November, when new vents formed extending the lower fissure to the southeast. The lava sourced from these new vents branched out into two flows, one to the southwest and the other to the south and southeast. The south-trending flow likely destroyed the Fuente Santa, at the time a popular medicinal spa. Few details are known after 26 November. During a fourth phase of activity, vents from the middle part of the lower eruptive fissure produced lava flowing to the west and southwest, widening the coastal platform to its present extent. Pyroclastic activity at the upper vent continued intermittently until at least 10 December. The eruption appears to have ended abruptly on 21 January.

3.4. The 1704–1705 eruption of Siete Fuentes, Fasnia, and Arafo, Tenerife

The 1704–1705 eruption on Tenerife originated from three distinct vents — Volcán de Siete Fuentes, Volcán de Fasnia and Volcán de Arafo — separated by a total of 10.4 km and aligned N40°E, essentially parallel to the northeast rift zone of the island (Fig. 3a). Siete Fuentes (2240 m altitude) is an elongated cinder cone, 30 m in height and 370 m in length, which produced three short lava flows, the southernmost of which was confined into a ravine and reached a maximum of 2.6 km from source. Fasnia (2180 m altitude) is a 45-m-high, 1300-m-long eruptive fissure which was the source of three short flows and one long, ravine-confined flow with a length of 6.4 km. Arafo (1490 m altitude) is a 100-m-high cinder cone that produced a complex lava flow field (Solana, 2012), with two longer branches reaching a maximum of 9.4 km from the vent. Published estimates of eruptive product area and volume respectively average at 5.2 $\pm$ 1.8 km^2 and 37 $\pm$ 22 $\times$ 10^6 m^3, whereas we obtain 4.6 km^2 and 37 $\times$ 10^6 m^3 (Tables 1–2, A.1–A.2). All three vents erupted basanitic products.

Our summary of this event is based on Solana (2012) and Albert et al. (2015, 2016) who reviewed historical accounts. The eruption

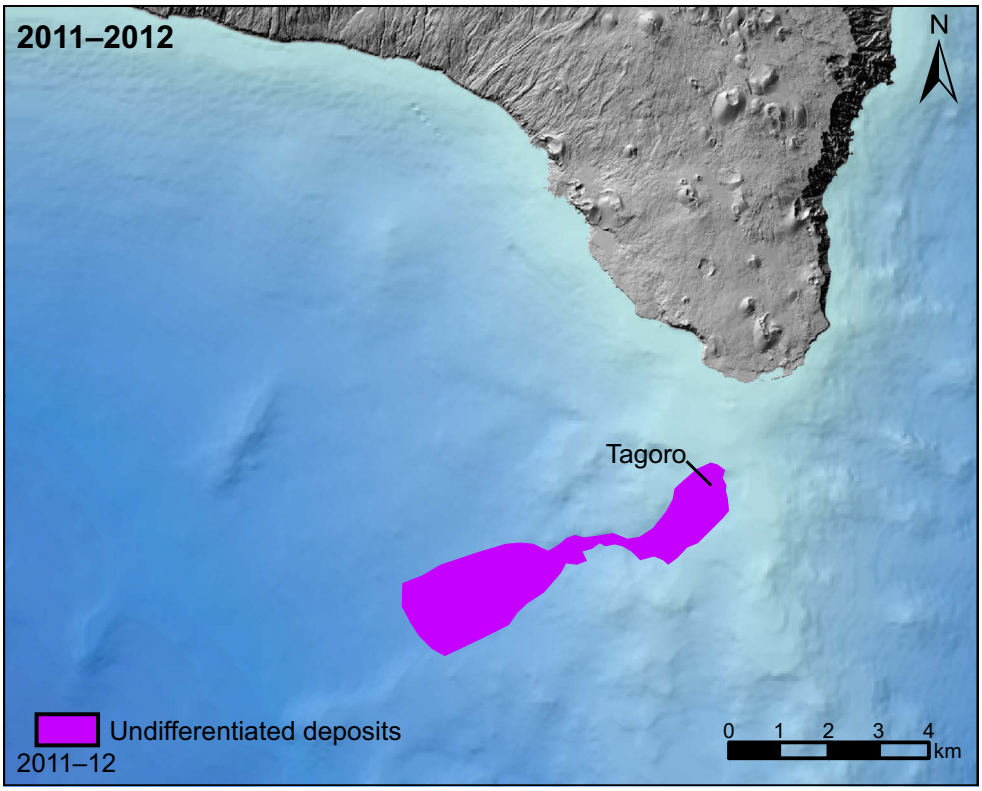

Fig. 5. Map of the 2011–2012 submarine eruption at El Hierro, modified after Rivera et al. (2013, 2014).

was preceded by seven days of felt seismicity and spanned a total of 86 days of discontinuous activity from 31 December 1704 to 27 March 1705 (Fig. 6d, Tables 1, A.6). Felt earthquakes also occurred throughout the eruptive period. Initial Strombolian and effusive activity at Siete Fuentes may have ended as early as 5 January, but no later the 16 January. On 5 January, a new eruptive fissure opened ~ 1 km to the northeast, forming the Fasnia vent. A brief explosive phase, of greater intensity than that at Siete Fuentes, was quickly followed by effusion of lava flows. Lava emission at Fasnia was reported to have lasted 12 days and had likely ended by 16 January. After a volcanic hiatus of 16 days, during which important seismicity occurred, eruptive activity resumed ~ 8 km northeast of Fasnia on 2 February, forming the Arafo vent. Again, this new eruptive phase appears to have begun explosively, with a greater intensity than the previous two phases. Indeed, the initial eruption column was reported visible from the town of La Orotava, which requires, based on the topographic profile between the town and the eruption site, that it reached heights of at least 1 km above the vent. Lava fountains ~ 30 m in height were reported on 11 February (Romero Ruiz, 1990). Although historical sources are unclear, the end of the eruption is taken as 27 March.

3.5. The 1706 Garachico eruption, Tenerife

The 1706 Garachico eruption occurred on Tenerife's northwest rift zone at ~ 1345 m altitude, building the 105-m-high Montaña Negra cone, also known as Volcán de Arenas Negras or Volcán de Garachico (Fig. 3b). The eruptive fissure is ~ 850-m long, trending N120°E. According to Solana (2012), the complex lava flow field associated with this eruption comprises four main flows, three of which reached the coast some 6.7 km downslope. Published values yield a mean planimetric deposit area of 7.9 ± 2.0 km^2, close to our result of 7.8 km^2. Volume estimates give 54 ± 8 × 10^6 m^3, while we obtain 76 × 10^6 m^3 (Tables 1–2, A.1–A.2). The eruption products show a basanite to tephrite composition.

The following eruption chronology is summarized from Solana and Aparicio (1999) and Solana (2012) who reviewed historical documents compiled by Romero Ruiz (1990). Additional details are provided by Carracedo (2013) and Romero Ruiz and Beltrán Yanes (2015). Beginning on 5 May 1706 and lasting approximately 40 days (ending around 13 June 1706), the 1706 eruption took place barely a year after, but more than 20 km away from, the 1704–1705 eruptive event (Fig. 6e, Tables 1, A.7). Historical accounts indicate that seismic activity continued after the end of the 1705 eruption up until the 1706 eruption, but felt seismicity is only specifically reported less than a day before eruption onset (Romero Ruiz, 1990; Sánchez, 2014). The eruption began at 3:30 am on 5 May 1706 with the opening of a fissure that produced lava flows rapidly advancing towards the coast first burying the village of El Tanque and then invading Garachico's natural harbor — at the time Tenerife's main port — only ~ 16 h after the eruption onset (Solana, 2012). The lava flow field continued expanding in the following week and, on 13 May, a secondary lava flow originating from a breached levee in the eastern part of the field cascaded down the cliff behind Garachico and destroyed its city center. Another branch of that flow also partially buried the village of San Juan del Reparo. Subsequent lavas remained proximal to Montaña Negra. Pyroclastic activity produced lapilli and ash that dispersed to the south–southwest up to 3 km from source. Solana and Aparicio (1999) quote an eruption column height estimate of ca. 1.5 km for the Garachico eruption.

3.6. The 1712 El Charco eruption, La Palma

The 1712 El Charco eruption occurred in the central part of Cumbre Vieja volcano, from an eruptive fissure totaling 2.5 km in length at the upper end of which a 700–1000-m-wide, ~ 95-m-high cone (Volcán del Charco or Montaña Lajiones) was built (Fig. 2d). Three main lava flow branches, which all reached the coast forming a wide platform, can be distinguished, with a maximum runout of 5.1 km. The only published value for proximal deposit area is 10.2 km^2 (Carracedo et al.,

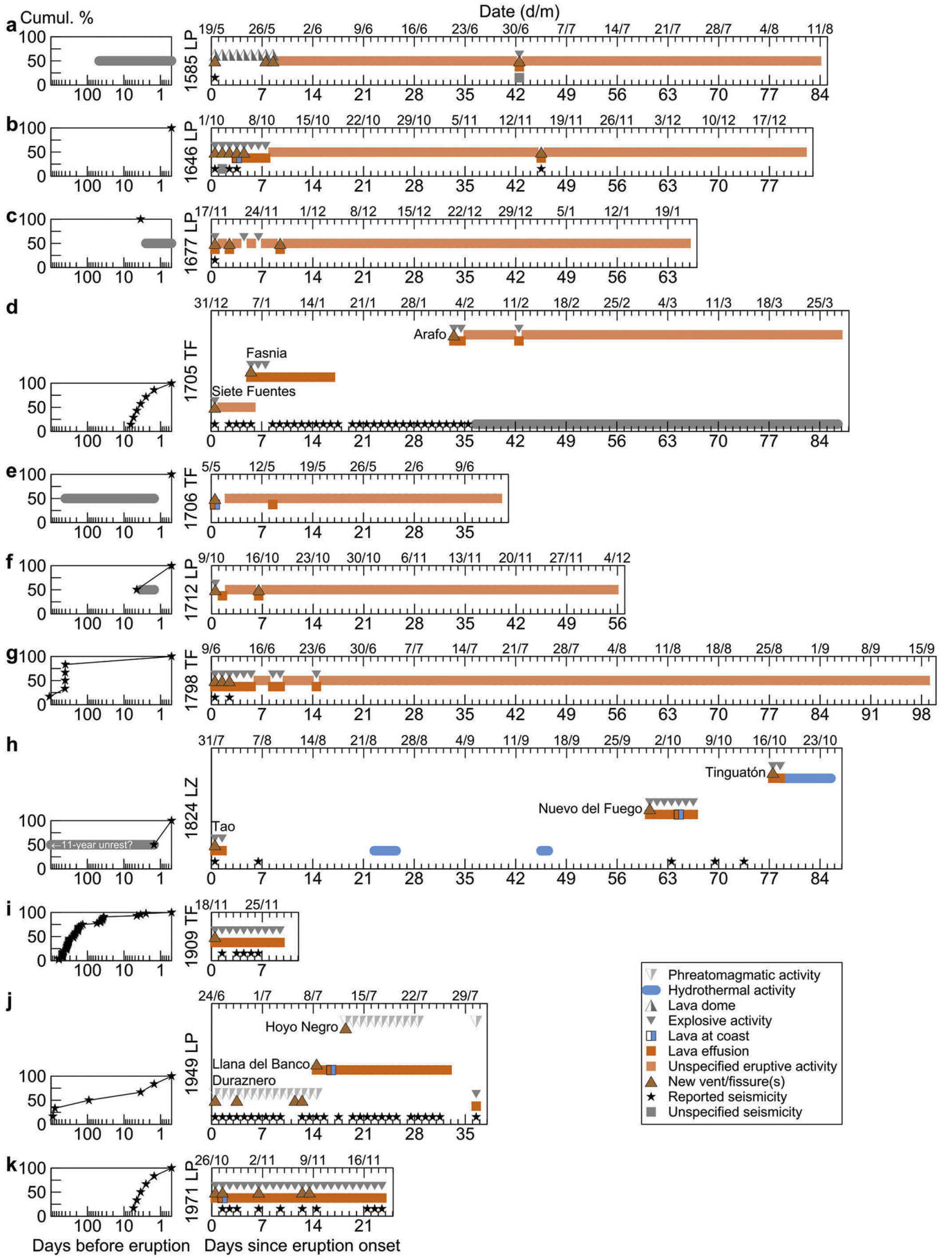
Cumul. %
Date (d/m)
a
1585 LP
b
1646 LP
c
1677 LP
d
1705 TF
Arafo
Fasnia
Siete Fuentes
e
1706 TF
f
1712 LP
g
1798 TF
h
1824 LZ
Tinguatón
Nuevo del Fuego
Tao
←11-year unrest?
i
1909 TF
j
1949 LP
Hoyo Negro
Llana del Banco
Duraznero
k
1971 LP
Phreatomagmatic activity
Hydrothermal activity
Lava dome
Explosive activity
Lava at coast
Lava effusion
Unspecified eruptive activity
New vent/fissure(s)
Reported seismicity
Unspecified seismicity
Days before eruption
Days since eruption onset

2015), which significantly exceeds our value of 4.5 km^2. Published values for eruptive volume average at $41 \pm 30 \times 10^6$ m^3; in comparison, we obtain 36×10^6 m^3 (Tables 1–2, A.1–A.2). Erupted magma composition is basanite to tephrite.

Historical sources describing this eruption are scarce and the following is briefly summarized from Romero Ruiz (1990). The eruption lasted 56 days from 9 October to 3 December 1712 (Fig. 6f, Tables 1, A.8). Felt seismicity is reported only 5 days before eruption onset. On 9 October, a fissure opened up in the upper part of the Cumbre Vieja rift with Strombolian explosive activity focusing at two vents. The following day, the lowermost vent began emitting lava flows, which descended towards the west coast. Then, on 15 October, the fissure extended further downslope in a northwest direction, producing effusive activity.

3.7. The 1730–1736 Timanfaya eruption, Lanzarote

The Timanfaya eruption on Lanzarote is highly anomalous in the context of historical Canary Island volcanism, as it dwarfs all other events in terms of duration, magnitude and impact, destroying 26 villages and forcing much of the population to flee the island. In fact, in the period since 1500 CE, it ranks second among the largest basaltic fissure eruptions globally, only surpassed by the 1783–1784 Laki eruption, in Iceland (Thordarson and Self, 1993). Ten main emission centers (and several more smaller ones) opened up sequentially, defining a ≥ 14.4-km-long eruptive fissure located centrally in the island's western sector (Fig. 4). Vent altitude and height range from 60 to 415 and 15–120 m, respectively, with some eruptive activity also likely taking place below sea level (Carracedo et al., 1992). The multi-branch lava flow field, mapped in detail by Carracedo and Rodríguez Badiola (1991), reached the island's northwest coast along a ~ 21-km-long perimeter and has a maximum end-to-end length of ~ 30 km. The longest runout distance for a single flow is 21.7 km (cf. Solana et al., 2004). Estimates of area covered by the 1730–1736 lava flows range from 150 to 226 km^2, with a mean of 187 ± 33 km^2 (Tables 1, A.1). However, it is unclear whether the higher end of those estimates also included a large lapilli field (La Geria) sometimes integrated in maps of the eruption's deposits. We obtain a lava flow area (i.e., excluding the lapilli field) of 146 km^2 (148 km^2 including vents, Table 2). Previous volume estimates vary from 1 to 5 km^3, with a mean of 2.5 ± 1.4 km^3 (Tables 1, A.2). Lava thicknesses reaching ~ 50 m can be observed, notably on the west coast, but are much thinner in other places at the edge of flow field. While poorly documented at present, mean lava thickness at Timanfaya is likely similar to that of better-constrained Icelandic lava flow fields, such as the 1783–1784 Laki eruption (599 km^2, 14.7 km^3, mean lava thickness of 25 m, (Thordarson and Self, 1993)) and the 2014–2015 Holuhraun eruption (82 km^2, 1.44 km^3, mean lava thickness of 17 m (Pedersen et al., 2017)). Integrating mean thicknesses of 15–25 m over an area of 146 km^2 yields a bulk lava volume of 2.2–3.7 km^3. In comparison, the empirical approach outlined in Section 4.5 gives 4.2 km^3. These estimates do not account for lava flows that entered the sea in large portions of the coastline, and so the true bulk eruption volume, including a significant tephra blanket (Muller, 2016), was likely larger. The Timanfaya eruption is also characterized by an unusual temporal trend in magma composition, from early high-MgO basanite giving way to tholeiitic basalt for most of its duration (Carracedo et al., 1990, see also companion paper).

Two main contemporary accounts of this eruption are known: the official reports of the Royal Court of Justice of the Canary Islands (Real Audiencia de Canarias, 1731) and the diary of Andrés Lorenzo Curbelo, the priest of the town of Yaiza, transcribed by von Buch (1825). Entries for these respectively end on and 12 April 1731 and 28 December 1731, and concrete information from 1732 to 1736 is extremely scant, which prevents a precise reconstruction of the eruption. Various authors (Carracedo, 2014; Carracedo et al., 1990, 1992; Carracedo and Rodríguez Badiola, 1991; Ortiz et al., 1986; Pallarés Padilla, 2007; Romero, 2003) previously reviewed these accounts. Fig. 7 is based on the reconstruction of Carracedo et al. (1990, 1992), with updates from Pallarés Padilla (2007) and Carracedo (2014), and our own review of contemporary sources (Tables 1, A.14).

According to historical sources quoted by Romero (2003), precursory seismic unrest may have begun by 1726, but no confirmed reports exist. The eruption commenced on 1 September 1730 and is thought to have ended on 16 April 1736 (duration of 2055 days), although the latter date has been questioned by Pallarés Padilla (2007) who argued the eruption ended a year earlier in 1735. The initial phase of the eruption involved three eruption centers: Caldera de los Cuervos (1–19 September 1730), Caldera de Santa Catalina (10–31 October 1730), and Pico Partido (10 October 1730 to January 1731). These vents produced extensive lava flow fields that destroyed several villages on their way to the northwest coast. In addition, historical records clearly indicate that these early eruptive episodes comprised significant explosive activity, with thick accumulation of lapilli and ash damaging roofs and ruining farmland. Eruption columns were high enough to allow ash to reach distal parts of Lanzarote and even the neighboring island of Fuerteventura (Carracedo, 2014; Romero, 2003).

After an apparent lull in activity of a few weeks, a second eruptive phase began forming Montañas del Señalo, nearby Pico Partido, and involved at least four distinct episodes between March and July 1731. Lavas emitted from Señalo travelled short distances to the north and southwest.

The onset of phase 3 is marked by a seemingly sudden shift of eruptive activity to the west coast, at a distance of at least 12 km from Señalo, at the end of June 1731. Historical accounts of explosions at the coast and occurrence of numerous dead fish on the shore indicate that this new phase likely initially involved submarine eruptive vents, and subsequently the subaerial Volcán El Quemado, a small elongated vent situated ~ 1 km from the coast. Continued migration of eruptive activity towards the east led to the formation of Montaña Rajada and Calderas Quemadas (a group of four closely-spaced cinder cones). These emission centers produced vast lava flow fields reaching the west coast.

At this point, the eruption had already had a strong impact on the island's infrastructure and farmland, which led to massive exodus of the islanders, and contemporary information on the eruption becomes very scarce. It is presumed that by early 1732, and for a prolonged but unknown period afterwards, the eruption focused at Montañas del Fuego, a large and complex cluster of overlapping cinder cones thought to have formed in the early explosive onset of this fourth phase. This activity, which may have discontinuously persisted until early 1736, also produced abundant lavas that flowed towards the northwest and southwest.

The fifth and last eruptive phase occurred 5 km east of Montañas del Fuego, at Montaña de las Nueces and Montaña Colorada, but the timing of its onset is uncertain. Lava emission at Montaña de las Nueces, which produced an impressive pāhoehoe lava flow that reached the coast near the town of Arrecife to the east, was originally thought to have taken place between mid-March and early April 1736 (Carracedo et al., 1992). Yet, a statement of Dávila y Cárdenas (1737), who visited Arrecife in February 1733, suggests that lava flows emitted from this vent already threatened the town's port at this time (Pallarés Padilla,

Fig. 6. Chronology of precursory and eruptive activity for historical Canary Island eruptions. Panels on the left show precursory felt seismicity on a logarithmic timeline. Black stars show the cumulative percentage of confirmed seismicity binned on a daily basis. Gray lines indicate periods where seismicity was reported to occur but not specified in time and occurrence. All eruption chronologies are shown on the same timescales in days since eruption onset on the lower x-axis. The upper x-axis shows corresponding calendar dates in d/m format of the given years. See Section 3 for symbology definitions. Chronologies for the 1730–1736 and 2011–2012 eruptions are presented in Figs. 7 and 8, respectively.

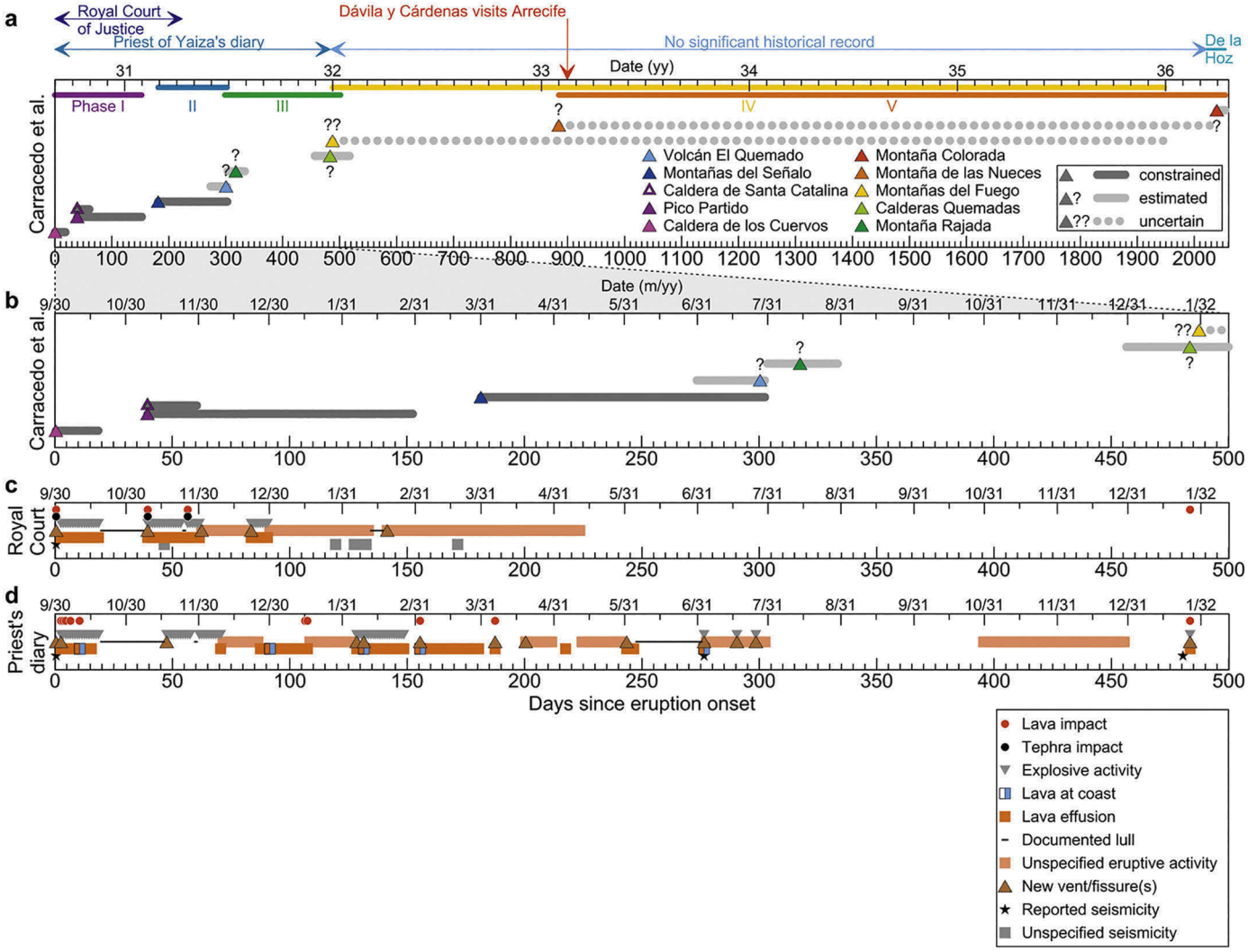

Fig. 7. Chronology of the 1730–1736 Timanfaya eruption, Lanzarote. For all panels, lower x-axes show days since eruption onset. Upper x-axes show corresponding calendar dates in yy for (a) and m/yy for (b–d). (a) The entire eruption timeline according to the reconstruction of Carracedo and Rodríguez Badiola (1991) and Carracedo et al. (1990, 1992), with updates from Pallarés Padilla (2007) and Carracedo (2014). The estimated duration of the five main eruption phases is shown by colored bars near the top of the plot. The onset and duration of activity of specific emission centers is shown by colored triangles and gray bands, respectively. These are either relatively well constrained from accounts (no additional symbol; dark gray band), estimated from accounts (?; light gray band), or involve large uncertainties (??; dotted light gray band). Blue arrows above the plot show the time spanned by the key historical documents. Note the lack of significant historical record for a duration of ~4 years from 1732 to 1736. A statement of Dávila y Cárdenas (1737), who visited Arrecife in February 1733 (red arrow), suggests that lava flows from Montaña de las Nueces already threatened the town's port at this time. (b) As in (a) but focusing on the first 500 days of the eruption, for which historical records are available. (c) Timeline of events according to the official reports of the Royal Court of Justice of the Canary Islands (Real Audiencia de Canarias, 1731). (d) Timeline of events according to the Priest of Yaiza's diary. For (c) and (d), symbols are as in Fig. 6, with the addition of documented lull in eruptive activity shown as solid black line and impact of lava flows and tephra fall on communities shown as red and black circles, respectively. (For interpretation of the references to colour in this figure legend, the reader is referred to the web version of this article.)

2007). If correct, this eruptive phase would then have started at least three years earlier than previously envisaged, illustrating the high level of uncertainty in the eruption's chronology beyond 1731. Finally, Montaña Colorada represents the last emission center of the Timanfaya eruption and appears to have been active for a short period in 1736, perhaps for only two weeks ending on 16 April 1736. This vent produced lava flows that fell short of reaching the sea to the north and a significant lapilli field on its south flank.

3.8. The 1798 Chahorra eruption, Tenerife

This 1798 Chahorra or Narices del Teide eruption occurred on the southwest flank of Pico Viejo volcano at ~ 2660 m altitude from a 1-km-long, NE–SW fissure, which formed the ~ 45-m-high Volcán de Chahorra vent cluster (Fig. 3c). The 1798 lava flows consist of two main branches: the largest one flowed down to 5.4 km to the south, but was confined by the Las Cañadas caldera wall, while the other one flowed west (Solana, 2012). Published and new estimates of proximal deposits area and volume match well (area: 4.5 ± 0.5 versus 4.6 km^2; volume: 30 ± 13 versus 37 × 10^6 m^3) (Tables 1–2, A.1–A.2). The eruptive products of this eruption have a phonotephrite composition, which is distinctly more evolved than all historical Canary Island lavas except the 1585 phonolite.

This eruption spanned at least 98 days from 9 June to 15 September 1798. Our eruption reconstruction follows the work of Solana (2012) (Fig. 6g, Tables 1, A.9). Historical accounts suggest that minor precursory seismicity might have begun 3 years prior to eruption (Romero Ruiz, 1990; Sánchez, 2014). However, there is a lack of record for clear seismic precursors in the days to months before eruption onset — a single earthquake is reported on 9 June as the eruption began. Syn-eruptive seismicity also appears to have been low. In the first 4 days of the eruption, the eruptive fissure migrated up the steep slopes of Pico Viejo from

2300 to 2800 m above sea level. Strombolian activity concentrated in the upper part of the fissure, while lava flows were mostly emitted from its lower part. The most explosive activity, possibly of violent Strombolian and/or phreatomagmatic character, appears to have taken place on 14 June, with eyewitness accounts estimating eruption column heights to 1–2 km. Beyond 23 June, no record of the continuing activity exists, and the exact end date of the eruption is uncertain.

3.9. The 1824 eruption of Tao, Nuevo del Fuego, and Tinguatón, Lanzarote

Lanzarote's 1824 eruption yielded the formation of three successive cinder cones, namely Volcán de Tao or del Clérigo Duarte, Volcán Nuevo del Fuego and Volcán de Tinguatón, aligned ENE–WSW and separated by a total of 14 km defining a lengthy, discontinuous fissure (Fig. 4). Located at the western end of the lineament, Tao (295 m altitude) is a small, elongated (700-m-long) cone, with a maximum height of 20 m, that produced short lava flows only extending 0.4 km. Nuevo del Fuego (330 m altitude) is a ~ 50-m-tall cone situated at the opposite, eastern end of the fissure and was the source of this eruption's main lava flow, which just reached the coast 6.3 km from the vent. Finally, Tinguatón (310 m altitude), located 4 km east-northeast of Nuevo del Fuego, is a 25-m-high cone that produced short lava flows extending up to 1.4 km. A single published value for deposit area of 5 km^2 (Carracedo et al., 2015) significantly exceeds our estimate of 2.8 km^2. Two published volume estimates are in poor agreement, with a mean of 11 $\pm$ 11 $\times$ 10^6 m^3 (Tables 1, A.2), whereas we obtain 19 $\times$ 10^6 m^3 (Table 2). Eruptive products have a basanitic composition.

Little has been published on this eruption; our reconstruction is based on Romero (2003), who reviewed historical documents (Fig. 6h, Tables 1, A.10). The discontinuous eruptive activity spanned 87 days from 31 July to 24 October 1824. Precursory seismicity may have begun as early as 11 years before eruption and is reported to have progressively increased in intensity and frequency in the months leading up to eruption. However, confirmed precursory earthquakes are limited to the two days preceding eruption onset and were accompanied by subterranean noises, ground cracking and gaseous emissions. A first eruptive fissure opened in the morning of 31 July near the towns of Tao and Tiagua and was characterized by mild Strombolian activity that produced both localized lava flows and pyroclastic ejecta, building the Tao cone. This magmatic activity rapidly declined and had ceased by 2 am on 1 August. From this point until 21 August, the activity was essentially reduced to gas emissions at the vent and seismic swarms felt by the population. Following the opening of new ground cracks, peculiar hydrothermal activity, apparently producing effusive emissions of brackish water through newly formed vents and cracks, occurred from 22 to 25 August and again from 14 to 15 September. On 29 September, a new eruptive phase began forming Volcán Nuevo del Fuego, which produced lavas and pyroclastics in amounts that rapidly exceeded those produced at Tao. Lava flows overlapped a small part of the 1730–1736 flow field and reached the coast on 3 October. The eruption intensity increased until 4 October, but suddenly diminished and had stopped by the next day. The time period between the end of activity at Nuevo del Fuego at the opening of the Tinguatón vent on 16 October was characterized by the occurrence of frequent seismic swarms and subterranean noises. Eruptive activity at Tinguatón began explosively, but effusive emission of localized lava flows shortly followed. This magmatic activity was of short duration and rapidly ended on 17 October, being quickly superseded by thick gaseous and hydrothermal emissions later on the same day. Contrasting with observations at Tao, hydrothermal emissions at Tinguatón were somewhat explosive, producing geyser-like jets reaching significant (although unreported) vertical extent. These emissions, unique in the context of historical Canary Island volcanism, lasted a week (until 24 October) and formed a series of aligned, deep and narrow pits on the Tinguatón crater floor visible on satellite images.

3.10. The 1909 Chinyero eruption, Tenerife

The most recent eruption on Tenerife occurred on the northwest rift zone of the island at ~ 1505 m altitude, forming the ~ 50-m-high Volcán del Chinyero located within a few kilometers of the 1706 cone (Fig. 3d). The total length of the eruptive fissure is ~ 500 m. The eruption produced a braided lava flow field comprising two main branches respectively extending north and west (Solana, 2012). The north branch reached 1.2 km from the vent, whereas the west branch, which was split in two as it encountered a topographic high, reached a maximum of 4.5 km from source. Previous proximal deposit area and volume estimate average at 2.0 $\pm$ 0.6 km^2 and 15 $\pm$ 8 $\times$ 10^6 m^3, respectively (Tables 1, A.1–A.2). In comparison, in Table 2, we list an area of 1.8 km^2 and a volume of 10 $\times$ 10^6 m^3. We note that Di Roberto et al.'s (2016) survey of pyroclastic deposits suggests that medial and distal tephra may significantly add to the eruptive volume (see details in Section 4.5). The composition of eruptive products is basanitic.

The following reconstruction of events is based on the accounts of Ponte y Cologán (1911) and Fernández Navarro (1911) and their summary by Solana (2012) and Di Roberto et al. (2016) (Fig. 6i, Tables 1, A.11). The eruption had a short duration of 10 days from 18 to 27 November 1909. Seismic activity felt by the island's inhabitants up to 19 months prior to eruption may represent early precursors (Albert et al., 2016). Within 17 h of the eruption onset, the activity involved up to nine vents aligned along a SE–NW fissure, but it soon focused at 3–4 emission points for the remainder of the eruption. The eruption began explosively with a pulsating, violent Strombolian phase that built the Chinyero cone within less than a day and lasted 4 days, causing significant fallout of lapilli up to 20 km and ash up to 130 km from the vent. Rough estimates of the maximum heights reached by glowing pyroclastic material during this phase range from 200 to 1000 m, with several estimates between 500 and 700 m. From the fourth day of the eruption, the intensity of the activity progressively decreased, although the eruption ended with a Vulcanian-style pulse producing abundant bombs and dense blocks. Throughout the eruption, emission of fine pyroclastic material was accompanied by lava effusion.

3.11. The 1949 San Juan eruption, La Palma

The San Juan eruption on La Palma took place in the central part of Cumbre Vieja volcano from three distinct vents (Duraznero, Llano del Banco, and Hoyo Negro), separated by a total of 3.3 km along the N–S rift zone (Fig. 2e). The eruptive fissure at Duraznero reached 400 m in length and built a 80-m-high cone situated at 1810 m altitude. Llano del Banco (1185 m altitude) is a 60-m-long eruptive fissure that did not build a cone, whereas Hoyo Negro (1880 m altitude) is a crater that pre-dated the 1949 event and is now ~ 100-m deep showing only about 20 m of positive topographic relief at its rim. The lava flow field at Llano del Banco comprises a single main branch 7.0 km long and 5–6 minor branches with a maximum length of 1.8 km. The main flow reached the west coast 7.0 km from the vent, forming a wide platform. Duraznero's lava flow was confined to a narrow ravine, travelling 7.1 km down the east flank of Cumbre Vieja, stopping only 30 m before reaching the coast. Carracedo et al. (2015) report a deposit area of 4.8 km^2, whereas we obtain 3.9 km^2. While most published volume estimates are consistent at ~ 22 $\times$ 10^6 m^3, Sobradelo et al.'s (2011) proximal tephra volume of 89 $\times$ 10^6 m^3, which appears too high, introduces significant scatter, yielding an overall mean of 51 $\pm$ 51 $\times$ 10^6 m^3 (Tables 1, A.2). In comparison, we obtain 29 $\times$ 10^6 m^3 (Table 2). The eruption was compositionally zoned, dominated by basanite but also producing tephrite and phonotephrite products (Klügel et al., 1999).

Notably, the 1949 eruption was accompanied by the formation of a system of ground cracks and faults, 2–3 km in length, clearly connecting the three eruption sites. Klügel et al. (1999) interpreted this fault system as the surface expression of a shallow dike, whereas Day et al. (1999)

argued it might represent incipient flank instability of Cumbre Vieja volcano.

Details on the chronology of this eruption, including impressive photographs, are presented by Bonelli Rubio (1950) and Romero Ortiz (1951), and are summarized by Klügel et al. (1999), which we follow here (Fig. 6j, Tables 1, A.12). Additional information from White and Schmincke (1999) is also integrated. The San Juan eruption had a complex temporal evolution spanning a total of 37 days from 24 June to 30 July 1949. Significant earthquakes occurring in 1936–1937 may represent precursors to the eruption, but felt seismicity occurred only sporadically in the next 12 years with two events recorded in January and May of 1947 (Klügel et al., 1999; Sánchez, 2014). Unambiguous seismic unrest began 91 days before the eruption and was strongest in the southern part of the island near the town of Fuencaliente (Albert et al., 2016; Sánchez, 2014). The eruption, which can be split into four phases, began near the pre-existing Montaña Duraznero with moderate phreatomagmatic explosions producing juvenile ash, lapilli and bombs, as well as lithics. During this first phase, which lasted two weeks, four new vents opened at Duraznero along a N—S fissure and dark eruption columns reached an apparent maximum height of ~ 1500 m on 6 July. The activity was accompanied by strong seismicity that impacted buildings in towns 4 km downslope. The abrupt cessation of activity at Duraznero and coincident opening of the Llano del Banco fissure marked the onset of the eruption's second phase on 8 July. Llano del Banco produced lava flows that reached the sea on 10 July and became less viscous at about the same time, resulting in efficient transfer of newly erupted lava towards the west coast at speeds of up to 10 m/s. On 12 July, while effusive activity at Llano del Banco continued, new vents opened at the base of the old Hoyo Negro crater and seismicity resumed, marking the beginning of a third eruptive phase. Phreatomagmatic explosions at Hoyo Negro recurred every few minutes, strongly modified the morphology of the old vent, and produced ballistic blocks and bombs as well as pyroclastic density currents from collapsing eruption columns that reached heights of ~ 700 m. After a peak in eruption intensity (30-m-high lava fountains at Llano del Banco and intense pyroclastic activity at Hoyo Negro) around 19 July, Hoyo Negro stopped erupting on 22 July whereas lava emission at Llano del Banco diminished gradually then stopped suddenly on 26 July. After a three-day lull, a final and brief (but vigorous) eruption pulse (fourth phase) occurred at Hoyo Negro and Duraznero on 30 July. While phreatomagmatic activity at Hoyo Negro reportedly rapidly ended that morning, Duraznero emitted lava fountains up to 100 m high, which fed a low viscosity lava flow that rapidly cascaded down towards the east in a narrow ravine, crossed a major road by mid-day, but subsequently slowed down and fell just short of reaching the sea.

3.12. The 1971 Teneguía eruption, La Palma

The most recent eruption on La Palma took place at relatively low altitude (~ 360 m) at the southern tip of Cumbre Vieja volcano, near the town of Fuencaliente and the 1677–1678 eruption site (Fig. 2c). Its location was closely associated with a prehistoric phonolite dome (Roque de Teneguía). The eruption initiated from an eruptive fissure ~ 200 m in length where the ~ 130-m-high Volcán Teneguía formed. Three main lava flow branches, to the southwest, south and southeast, covered part of the 1677–1678 lavas and all reached the shoreline, forming coastal platforms. The maximum flow path of the southeast flow is ~ 2.7 km. Published and new planimetric area estimates of proximal eruption deposits are 3.7 ± 0.8 and 3.0 km^2, respectively (Tables 1–2, A.1). With pre-eruption topography known, the volume (40×10^6 m^3) and average lava flow thickness (12 m) of the 1971 eruption are better constrained than for most other historical Canary Island eruptions (Afonso et al., 1974) (Tables 1–2, A.2). Erupted products have a basanitic to tephritic composition.

The eruption was well observed and described in a dedicated volume of *Estudios Geológicos* (e.g., Afonso et al., 1974; Araña and Fuster, 1974) (Fig. 6k, Tables 1, A.13). It lasted 24 days from 26 October to 18 November 1971. Reported precursory seismicity started only 6 days prior to eruption (Albert et al., 2016; Sánchez, 2014). An eruptive fissure first opened up, producing pyroclasts and lavas that reached the coast on 27 October. The Teneguía cone began growing at the north end of the fissure and comprised five distinct emission centers that opened up sequentially. The latest vents, which became active on 7 and 8 November, produced more explosive Strombolian activity, with lava fountains reaching 200 m in height, and lower viscosity lava flows. Sizable bombs, frequently reaching 50 cm across, were projected up to 450 m from source (Fernández Santín et al., 1974). Finer tephra was primarily dispersed to the southeast and southwest of Teneguía and reached thicknesses of ~ 5 cm at the coast (Afonso et al., 1974). Explosive and effusive activity ended rather abruptly on 18 November.

3.13. The 2011–2012 Tagoro submarine eruption, El Hierro

The first historical eruption at El Hierro occurred at shallow water depths about 2 km off the south coast of the island (Fig. 5). While eruptive activity could not be directly observed, repeated, high-resolution bathymetric and hydroacoustic surveys during the eruption and subsequent remotely operated vehicle (ROV) observations allowed capturing the development of the submarine volcano and its associated volcaniclastic debris and lava aprons (Rivera et al., 2013, 2014; Somoza et al., 2017) (Fig. 8b). The submarine cone, which was later named Volcán Tagoro, grew from initial water depths of ~ 360 m to just 88 m below sea level. It is an elongated cone showing evidence for four distinct vents aligned NNW–SSE along a 500-m-long sloping ridge (Rivera et al., 2013, 2014). Its deposits followed a submarine canyon to the west-southwest, forming proximal and distal aprons at 500–850 and 1000–1800 m below sea level, respectively, and reached 7.0 km from source. Carracedo et al. (2015) report a deposit area of 5 km^2, while we obtain 6.9 km^2. Rivera et al. (2013) estimated the bulk volume of erupted material to 329×10^6 m^3 (Fig. 8b, Tables 1–2).

The 2011–2012 eruption was intensely monitored and was the subject of numerous multi-disciplinary studies, which we unfortunately cannot all cite here. The reader is referred elsewhere for more extensive summaries (Carracedo et al., 2015; González et al., 2013; Longpré et al., 2014; Martí et al., 2013a, 2013b; Meletlidis et al., 2015; Somoza et al., 2017). The first clear precursors were detected on 7 July 2011, 96 days prior to the onset of eruptive activity, and consisted of ground deformation measured by GPS and low-magnitude volcano-tectonic earthquakes located in the north-central part of the island (López et al., 2012) (Fig. 8a, Table A.15). Time series of diffuse CO_2 and H_2S soil efflux measurements also showed precursory signals (Pérez et al., 2012). Volcano-tectonic seismicity began migrating towards the south in September, intensified, and was accompanied by shifting ground deformation patterns; this unrest culminated with the appearance of volcanic tremor on 10 October, which is interpreted to mark the beginning of eruption (López et al., 2012). After a 10-day period of decreased earthquake activity, a seismic swarm began to the north of El Hierro (centered some 15–20 km from the eruption site), lasting until the end of November 2011 (Longpré et al., 2014; Martí et al., 2013a) (Fig. 8a). Minor seismicity occurred again in January and February 2012 before authorities declared on 5 March that the eruptive phase had ended. However, a marked change in seismic waveform similarity suggests the end of eruptive activity on 15 February (Sánchez-Pastor et al., 2018), yielding an eruption duration of 128 days.

At the surface, observations of seawater discoloration patches beginning on 12 October south of La Restinga village confirmed the approximate location of the eruption site. On 15 October, peculiar eruptive products reached the surface floating on water and were characterized by a black crust 1–2 cm thick and a pumice-like gray to white core (e.g., Troll et al., 2012). On 5–8 November, particularly intense degassing episodes produced large gas bubble bursts reaching up to 15 m above sea level (Meletlidis et al., 2015). Starting in mid-

November, but particularly in late November and early January, hollow lava balloons (e.g., Kueppers et al., 2012), up to 1–2 m across and with a basanite composition, were frequently observed temporally floating above the vent (Meletlidis et al., 2015) (Fig. 8b, Table A.15).

Remarkably, after the end of the eruption, a total of six temporally and spatially discrete seismic swarms occurred, associated with marked island-scale ground deformation pulses, the first one in June 2012 and the last one in March 2014 (Benito-Saz et al., 2019; Klügel et al., 2015). These events were interpreted to record distinct magma intrusions at upper mantle to lower crustal depths that did not culminate in eruptions. Domínguez Cerdeña et al. (2018) and Benito-Saz et al., 2019 respectively estimated that these post-eruptive intrusions emplaced a total volume of 361 and 388 $\times$ 10^6 m^3 of dense magma at depth, which exceeds dense rock equivalent estimates of erupted magma volume (Longpré et al., 2017) by a factor of 1.4–2.4. These observations demonstrate that magmatic activity beneath Canary Island volcanoes may involve rapid migration of magma over tens of kilometers laterally.

4. Eruption parameters

In this section, a broader discussion of the key physical eruption parameters listed in Tables 1 and 2 is presented, keeping in mind the end goal to inform hazard assessment.

4.1. Fissure length

Historical Canary Island eruptions typically began by the opening of a fissure several hundred meters in length. In most cases, eruptive activity focused at a main vent or vents, usually located at higher elevations along this initial fissure. However, in several other cases (most notably in 1704–1705, 1730–1736, 1824 and 1949), new vents opened up at significant distances from the initial fissure in subsequent eruptive phases. Lengths listed in Table 2 reflect the final vent-defined and sometimes discontinuous fissures — for discontinuous fissures, this assumes that distant vents are somewhat linked to each other in the shallow subsurface through the propagation of a dike. Values range from 200 m to 14.4 km. The two longest fissures formed during eruptions on Lanzarote, which may be related to the local stress field, but eruption phases involving distant vents are clearly possible on other islands too (e.g., the 1704–1705 Tenerife eruption).

4.2. Eruption column height

Data on eruption column height are required to accurately assess eruption style and explosivity, but unfortunately few are available for the eruptions studied herein. Direct observations of the 1971 La Palma eruption recorded maximum lava fountaining heights of 200 m (Araña and Fuster, 1974), while glowing pyroclasts reached 500–700 m during the 1909 Tenerife eruption (Di Roberto et al., 2016). However,

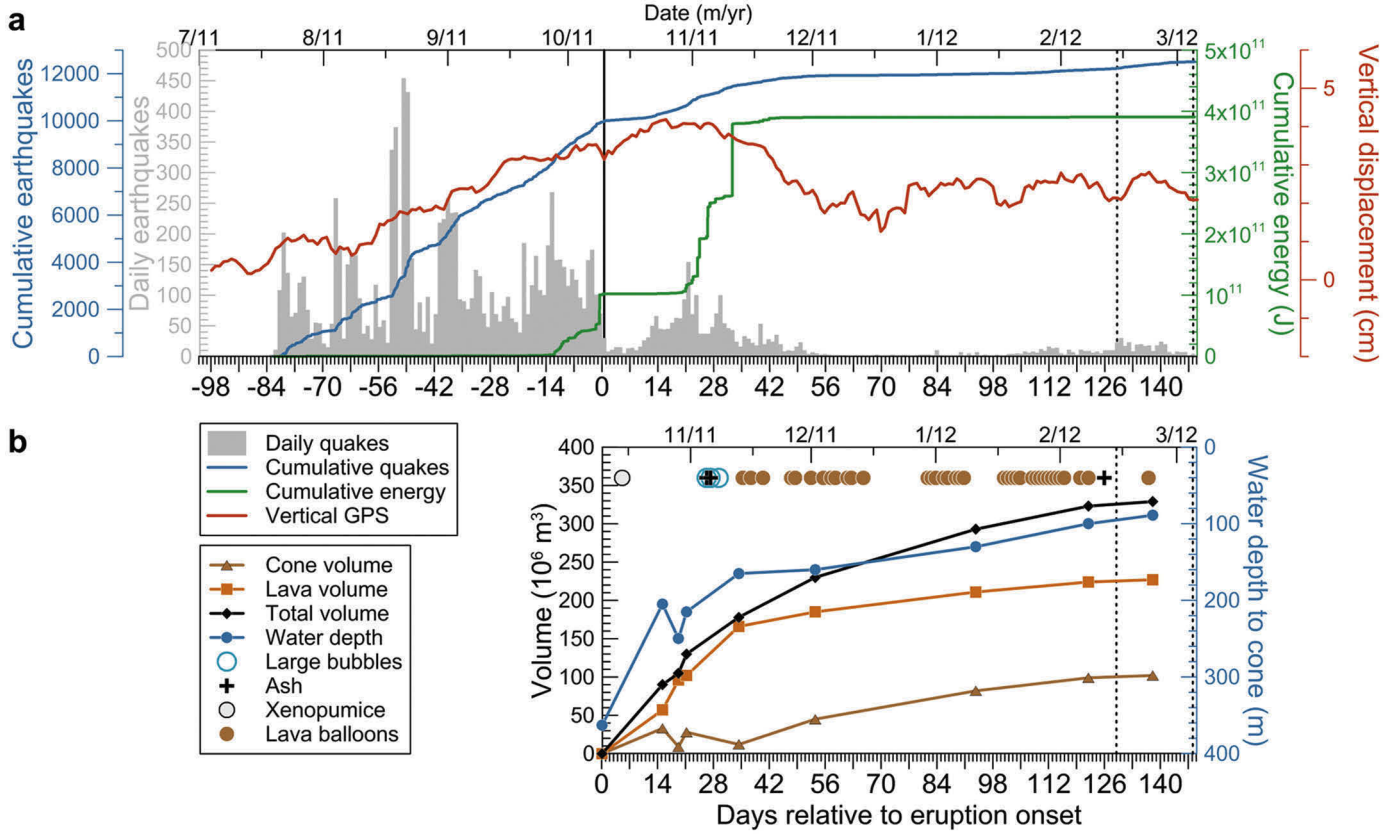

Fig. 8. Chronology of the 2011–2012 Tagoro eruption, El Hierro. For both panels, lower x-axes show days relative to eruption onset and upper x-axes show corresponding calendar dates in m/yy. (a) Geophysical monitoring data of precursory unrest and eruptive activity; the daily number of earthquakes is shown as a gray histogram, whereas the blue and green lines show the cumulative number of earthquakes and associated cumulative release of energy, respectively. The red line shows the 7-day moving average of the vertical component of the FRON continuous GPS station (e.g., Benito-Saz et al., 2019). The eruption onset and end are shown as vertical solid and dashed black lines, respectively. (b) Summary of bathymetric data quantifying submarine volcano growth (Rivera et al., 2013) and observations of eruption-related products at the surface (Meletlidis et al., 2015). Cone (brown triangles), lava flow (and associated debris apron, orange squares), and total (black diamonds) eruptive volumes are shown. Water depth to the cone summit is shown by blue circles and reached a minimum of 88 m below sea level. The earliest eruptive products, termed xenopumice (gray circle), reached the surface on 15 October, but were superseded by ash and scoria (black cross), intense degassing episodes (open blue circle), and, starting in November, lava balloons (brown circles).

more explosive phreatomagmatic pulses producing ash-laden eruption columns reaching 1–2 km seem to have occurred at least in 1704–1705, 1706, 1798 and 1949 (see photographs by Bonelli Rubio, 1950). No contemporary estimates of column height exist for the 1730–1736 Lanzarote eruption, but unpublished tephrostratigraphy work suggests it may have exceeded several kilometers in the first phase of the eruption (Muller, 2016). There is fertile ground for future tephrostratigraphy work in the Canaries to better constrain the dynamics of explosive eruption phases.

4.3. Lava flow length

The length reached by lava flows is another important variable for hazard assessment and it is relatively straightforward to measure for historical Canary Island eruptions. Table 2 lists two values per eruption: L_1 — the maximum lava flow length along the main flow path, and L_2 — the maximum length of the lava flow field from source to toe taken in a straight line. L_1 values, which are typically longer than L_2 values, are those reported in Section 3. In an extreme example, the Montaña de las Nueces lava flow field from the 1730–1736 Timanfaya eruption has a L_1 value of 21.7 km (cf. Solana et al., 2004) and a L_2 value of 15.7 km. L_1 and L_2 values show full ranges of 2.7–21.7 and 2.4–15.7 km, respectively. Excluding the 1730–1736 eruption, mean lava flow length maxima (L_1) are 5.5 ± 1.9 km (L_2 yields 5.3 ± 1.9 km). However, for three quarters of the eruptions, the longest lava flows reached the coast and therefore likely did not attain their maximum potential length over ground. Lavas that did not reach the sea in 1704–1705, 1798 and 1909 have a slightly longer mean maximum length of 6.4 ± 2.6 km. We consider this latter value plausible for future subaerial eruption scenarios for vents relatively distal from the coast, with only a low probability of lava runout exceeding 11.7 km (two standard deviations above mean) from source. We also note that lava flows may reach their full length and coastal areas rapidly, within hours to days of the onset of emission (Solana, 2012) (Fig. 6).

It may be informative to compare observations with the theoretical models of Kilburn (2004, 2015) that allow prediction of the maximum length of `a`ā flows as a function of ground slope and mean lava discharge rate. Fig. 9 shows the length of historical lava flows from the Canaries, along with single `a`ā flows at Etna, Kīlauea and Mauna Loa volcanoes, as a function of these variables. Overall, Canary Island lavas conform to the models and fall within the field of other basaltic lavas (cf. Solana, 2012). There are, however, significant uncertainties in the mean discharge rate, which is simply taken as the quotient of the mean lava volume estimate and eruption duration (Table 1). A particularly interesting case is again that of the 21.7-km-long Montaña de las Nueces lava flow that shows pāhoehoe surface morphology (Solana et al., 2004) and thus may not be expected to obey `a`ā flow behavior. Using a lava volume of 140 ± 30 × 10^6 m^3 and an eruption episode duration of 2–4 weeks (Carracedo et al., 1992; Solana et al., 2004), a mean discharge rate of 77 m^3/s is obtained, consistent with data from `a`ā flows (Fig. 9). However, based on historical records reported by Pallarés Padilla (2007) (see Section 3.7, Fig. 7a), emplacement of this lava flow field may have had already begun by February 1733 (i.e., for an eruption duration of possibly more than three years), which, if correct, dramatically reduces the mean discharge rate to <1.4 m^3/s and displaces the data point outside of the cluster for `a`ā flows (Fig. 9). Such protracted eruption duration at Montaña de las Nueces would also propagate into a much slower lava advance rate than previously envisaged by Solana et al. (2004).

4.4. Lava flow area

Table 2 reports planimetric area values for lava flows (A_L) and total proximal deposits (A_T), which include lavas and vents built of pyroclastic material, but exclude medial to distal tephra blankets. These measurements, computed using the ESRI ArcMap software, are precise and their accuracy is controlled by that of lava flow field delineation in the IGME geologic maps. A_T ranges from 1.8 to 7.8 km^2, with a mean 4.3 ± 1.7 km^2. As for lava flow lengths, area values are minima for eruptions reaching the coast. Fig. 10a compares area estimates from this and previous works. Although the agreement between studies is generally reasonable, there are significant discrepancies, e.g., for the 1712 eruption, the cause of which is unknown but may relate to the choice of maps and/or the chosen convention on incorporation/exclusion of pyroclastic material. As noted in Section 3.7, the significant mismatch between the mean published value (187 ± 33 km^2) and ours (148 km^2) for the 1730–1736 eruption is likely due to inclusion of La Geria, a wine-producing valley covered with a thick tephra blanket, in some of the literature estimates.

4.5. Lava flow and eruptive volume

Eruptive volume is a particularly useful parameter in a number of volcanological applications, such as determination of eruption magnitude (Pyle, 2015) and magma supply/output rates (e.g., Dvorak and Dzurisin, 1993; White et al., 2006). Unfortunately, it is also notoriously difficult to estimate (Pyle, 2015). For lavas, volume can be precisely and accurately determined if pre-eruption topography is known (e.g., Murray and Stevens, 2000). When pre-eruption topography is unknown, however, volume estimates rely on sparse lava thickness measurements typically at the edge of the flow field, which may not be representative of the mean flow thickness. In the Canaries, quantitative data on pre-eruption topography only exist for the 1971 La Palma and 2011–2012 El Hierro eruptions. Bulk volume (i.e., not corrected for porosity) estimates of these eruptions are respectively 40 × 10^6 m^3 (Afonso et al., 1974) and 329 × 10^6 m^3 (Rivera et al., 2013) and include both the vents and lava flows. For the 1971 eruption, the value of 31 ± 13 × 10^6 m^3 listed in Table 1 is a mean affected by a lower value reported by Sobradelo et al. (2011) who did not consider pre-eruption topography. Estimates for other eruptions (excluding 1730–1736, 1971 and 2011–2012) range from 11 to 66 × 10^6 m^3, with a mean of ~ 35 ± 18 × 10^6 m^3, but are likely subject to significant uncertainties (Tables 1, A.2). Indeed, except from a few exceptions (e.g., Sobradelo et al., 2011; Solana, 2012), the method of estimation is typically not reported and it is unclear whether volumes include vents or account only for lavas. We note that estimates in Table 1 also exclude medial to distal tephra blanket volumes, which may be significant but are unknown for all but the 1909 eruption. For this event, Di Roberto et al. (2016) estimated a bulk tephra volume of 15 × 10^6 m^3 (4–6 × 10^6 m^3 dense rock equivalent — DRE), which is similar to the bulk lava flow volume of 15 ± 8 × 10^6 m^3 (13 ± 7 × 10^6 m^3 DRE) (Tables 1, A.2). To sum up, bulk proximal deposit volumes listed in Table 1 likely represent minimum eruption volumes, for which uncertainty may be very high in certain cases. More robust eruption volume estimates will necessitate detailed field surveys of lava flow and tephra deposits (e.g., Di Roberto et al., 2016).

In the meantime, we develop a new empirical approach inspired from Murray and Stevens (2000) to calculate lava volume based on the assumption that lava flow area, which is precisely determined, is the best available proxy for volume. This approach exploits lava flow area and volume data for eruptions at other basaltic volcanoes for which volume estimates were derived from subtracting well-constrained pre-eruption topography from post-eruption topography and are thus likely substantially more precise and accurate. These data include 32 eruptions at Mount Etna, from 1879 to 1991 (Murray and Stevens, 2000) and 1999–2006 (Tarquini and Favalli, 2011), the 1995 (Amelung and Day, 2002) and 2014–2015 (Bagnardi et al., 2016) eruptions of Fogo volcano (Cape Verde), the 2014–2015 Holuhraun eruption (Iceland) (Pedersen et al., 2017), the 2018 Lower East Rift Zone eruption at Kīlauea (Neal et al., 2019), and 25 eruptions at Piton de la Fournaise from 1998 to 2017 (Derrien, 2019). This dataset, which spans areas of 0.15–84 km^2 and volumes of 0.5–1440 × 10^6 m^3, displays a positive

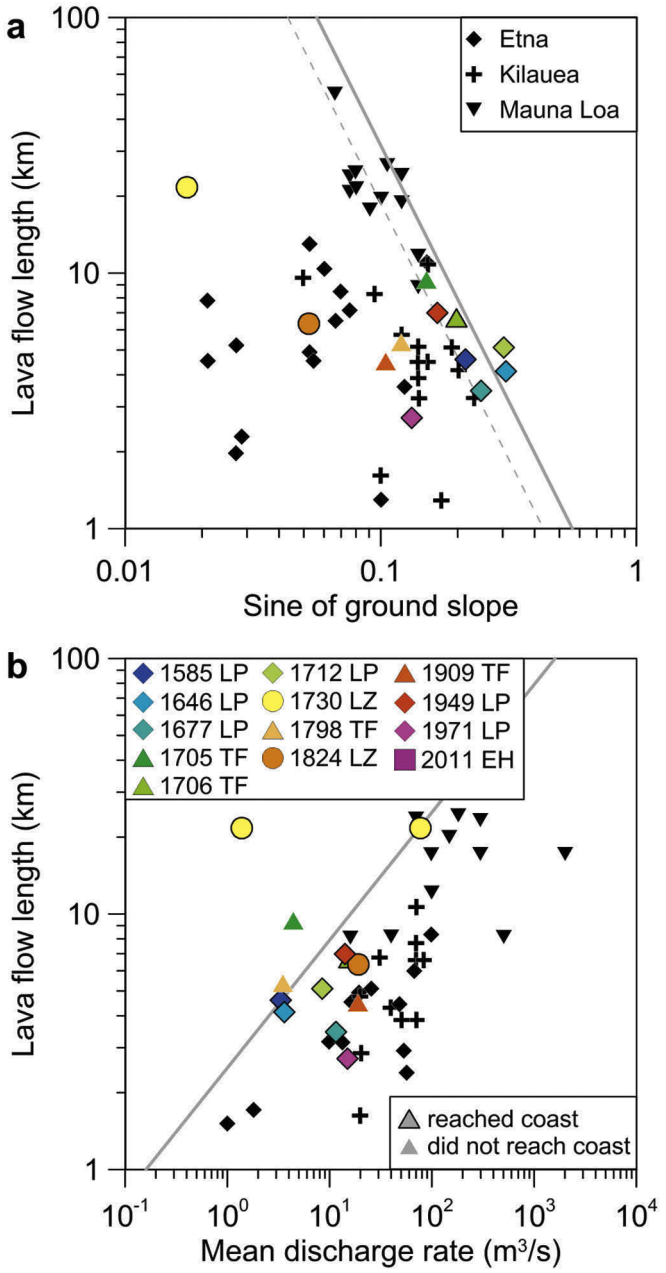

Fig. 9. Length of historical Canary Island lava flows. (a) Lava flow length versus the sine of ground slope. The dashed and solid lines represent the theoretical maximum length of `a`ā lava flows calculated with Eq. 23 and Eq. 27 of Kilburn (2004), respectively. (b) Lava flow length versus the mean discharge rate. For eruptions dominated by a single vent, the mean discharge rate was coarsely obtained by dividing the mean volume estimate by the eruption duration (Table 1). For eruption involving multiple separate vents (1704–1705, 1730–1736, 1824 and 1949) the discharge rate was obtained for the episode producing the longest lava flow only; e.g., for the 1704–1705 eruption, the volume and duration of the Arafo episode were used to calculate mean discharge. For the 1730 eruption, two points are shown for the Montaña de las Nueces episode to account for its uncertain duration (Carracedo, 2014; Carracedo et al., 1992). A high discharge rate of 77.3 m^3/s is obtained using a 21-day duration; a low discharge rate of 1.4 m^3/s is obtained using a 1170-day duration. The theoretical maximum length of `a`ā lava flows calculated with Eq. 55.1 of Kilburn (2015) is shown by the solid line. In both panels, line style around symbols for Canary Island data points indicates whether lavas have reached the coast; only lavas of the 1704–1705, 1798 and 1909 Tenerife eruptions did not. The 2011–2012 submarine eruption is omitted from these plots. Data for single `a`ā flows from Etna, Kīlauea, and Mauna Loa are shown for comparison (Kilburn, 2004, 2015 and references therein).

correlation on a log–log volume versus area diagram (Fig. 10b). A least squares linear fit through these data and forced through the origin yields Eq. 1:

$$V = 17.47A \quad (1)$$

where V is lava volume in millions of cubic meters (10^6 m^3) and A is lava area in km^2. Equation 1 has a high coefficient of determination (R^2 = 0.97), but this is strongly controlled by the two largest events (the 2014–2015 Holuhraun and the 2018 Kīlauea eruptions). This results in a relatively large standard error of estimate of 40 × 10^6 m^3 and a significant overestimation of volume for small flows. A power law fit (Eq. 2) yields a lower R^2 (0.88), but a much better standard error of estimate of only 2 × 10^6 m^3 and is thus preferred:

$$\ln(V) = 1.37\ln(A) + 1.52 \quad \text{or} \quad V = 4.56A^{1.37} \quad (2)$$

Lava volumes for Canary Island eruptions obtained with Eqs. 1 and 2 are given in Table 2 and Eq. 2 values are compared with published estimates in Fig. 10c and d. Despite some scatter about the one-to-one line, calculated volumes fall within one standard deviation of the mean published estimates in most cases (Fig. 10c, d). Since our model is based on subaerial basaltic lavas, it is unlikely to be valid for submarine lava flows, which differ in their emplacement dynamics (e.g., Gregg and Fornari, 1998), and thus it cannot be applied to the 2011–2012 eruption. For the only other event with known pre-eruption topography — the 1971 eruption — we obtain 21 × 10^6 m^3 which is about half the preferred value of 40 × 10^6 m^3 (Afonso et al., 1974). For the 1730–1736 Timanfaya eruption, lava volumes of 2.6 and 4.2 km^3 are obtained with Eqs. 1 and 2, respectively, consistent with the mean of published estimate of ~ 2.5 ± 1.4 km^3, although such values fall outside the calibration range of the model.

While clearly approximate, our empirical model (Eq. 2) could be useful for estimating volumes for small- to medium-sized basaltic lava flows elsewhere, when pre- and post-eruption topography is unknown and/or field-exposure of lava thicknesses is poor. We note that this model does not apply to confined lava flows, e.g., located within a crater or a narrow ravine, and we caution against its extrapolation for large lava flows.

5. Eruptive rate and long-term eruption forecasting

The volume estimates presented in Section 4.5 (Tables 1–2, A.2) allow to approximate eruptive rates for the 1585–2020 period. For the entire archipelago, mean published volume estimates, as well as values obtained from Eqs. 1 and 2, yield eruptive rates ranging from 7.3 to 11.0 × 10^6 m^3/year (Fig. 11a). Excluding the Timanfaya eruption, these values drop to 1.0–2.1 × 10^6 m^3/year, including 0.4–1.0 × 10^6 m^3/year at Cumbre Vieja volcano alone (Fig. 11a inset, b). These calculations help illustrate the extremely low magma supply at Canary Island volcanoes compared to other more vigorous ocean island shield volcanoes. Indeed, for context, eruptive rate at Kīlauea volcano alone is typically 80–100 × 10^6 m^3/year (e.g., Dvorak and Dzurisin, 1993), about a factor of 10 greater than our highest estimate for the entire Canary Archipelago. Of course, eruptive rate does not equate magma supply rate, which is likely higher given the evidence for significant endogenous island growth (Benito-Saz et al., 2019; Klügel et al., 2015). In this regard, it is interesting to compare historical eruptive rates with long-term eruptive rates, which are obtained independently by the quotient of volcano volume and age and, as such, should be representative of long-term magma supply. For instance, at Cumbre Vieja, the long-term eruptive rate is ~ 1.0 × 10^6 m^3/year (125 km^3 over 125 ka) (Carracedo et al., 1999a). At El Hierro, eruptive rates of 0.1–0.6 × 10^6 m^3/year are obtained considering the current subaerial island volume of 140 km^3, plus up to 500 km^3 of rock lost to giant landslides, and an age of 1.12 Ma (Carracedo et al., 1999b). Considering the completely different spatial and temporal scales used in both calculations, the agreement between historical and long-term eruptive rates is quite remarkable. It suggests that magma supply to Canary

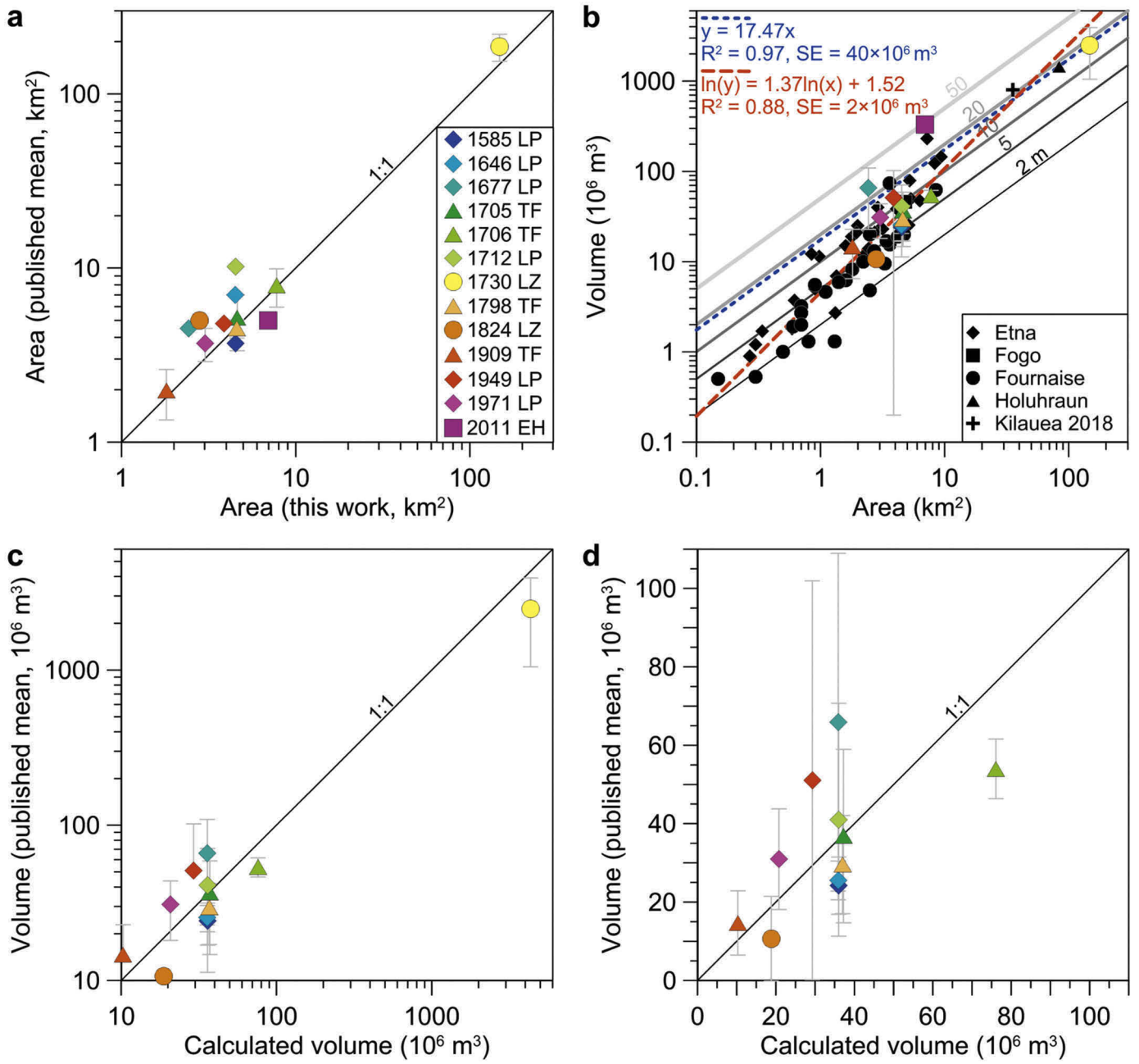

Fig. 10. Estimates of lava flow area and volume for historical Canary Island eruptions. (a) Mean published estimates of lava flow area compared to those obtained in this work. (b) Estimates of lava flow volume versus area. For Canary Island eruptions, mean published volumes are shown with 1σ error bars. Black symbols report data from eruptions at other basaltic volcanoes for which volume was derived from well-constrained pre- and post-eruption topography. Data sources: Etna: Murray and Stevens (2000), Tarquini and Favalli (2011); Fogo: Amelung and Day (2002), Bagnardi et al. (2016); Piton de la Fournaise: Derrien (2019); Holuhraun: Pedersen et al. (2017); and Kīlauea, 2018: Neal et al. (2019). The blue and red dashed lines represent linear (Eq. 1) and power law (Eq. 2) fits, respectively, through the black data points only, and are reported with associated equation, coefficient of determination (R^2) and standard error of estimate (SE, in millions of m^3). Black to gray lines show lava flow isopachs of 2, 5, 10, 20 and 50 m. (c) Mean published field-based volumes compared with calculated volumes based on the power law Eq. 2 derived in (b). The 2011–2012 event is omitted as Eq. 2 does not apply to submarine eruptions. (d) As in (c), but excluding the 1730–1736 eruption. Note the log–log scales in (a–c) and linear scale in (d).

Island volcanoes is relatively consistent over time and is reasonably well represented by the historical period.

In turn, this brings the question: can the historical record be used to construct decadal–centurial eruption forecasting models? Treating the 1704–1705 and 1706 eruptions as a single event, repose periods (r_1) listed in Table 1 give a mean eruption recurrence interval of 39 ± 24 years in the Canaries. For La Palma, repose has ranged from 22 to 237 years, with a mean 77 ± 91 years. Based on a slightly different eruption list including unconfirmed events, Araña et al. (2000) used the method of De la Cruz-Reyna (1993) and obtained 95%-confidence recurrence intervals of 26–41 years for the archipelago and 44–83 years for Tenerife only. In turn, Sobradelo et al. (2011) used extreme value theory and statistical analysis to calculate probabilities of occurrence of future eruptions as a function of eruption magnitude and time. They generally obtained high probabilities of occurrence (53–99%) in the next 20 years for the range of magnitude considered (M1 to M4). Coincidently, this study, which also noted the non-negligible probability (28%) of occurrence of a M > 1 eruption in the following year, was published within days of the onset of the 2011–2012 eruption.

Here we revisit long-term eruption forecasting in the Canaries by testing the historical eruption sequence for potential time-predictable or volume-predictable behavior (as defined by Marzocchi and Bebbington, 2012), which has been documented at several volcanoes (e.g., Burt et al., 1994; Hill et al., 1998; Sandri et al., 2005; Wadge, 1982). We adopt the approach outlined by Sandri et al. (2005) to test for a significant positive correlation between (1) the volume of an eruption and the subsequent repose period (time-predictable) and (2) the repose period and the volume of the subsequent eruption (volume-predictable). Three scenarios were considered for each case (Fig. 12, Tables A.16–A.17). The first one uses the repose period since the onset of the previous Canary Island eruption (r_1, Table 1), but considers the 1704–1705 and 1706 eruptions as a single event and excludes the 1730–1736 Timanfaya eruption (Fig. 12a, d). This scenario essentially treats the Canary Islands as interdependent volcanic systems, which could be consistent, for example, with a broad, blob-type mantle plume (Hoernle and Schmincke, 1993) governing magma generation and supply at the archipelago scale. The second and third scenarios use the repose period since the onset of the previous eruption on a given island (r_2, Table 1), thus considering each island as a separate system with independent magma supply, and respectively utilize the full eruption sequence (Fig. 12b, e) and focus on Cumbre Vieja volcano on La Palma (Fig. 12c, f). The results of this analysis reveal a lack of significant positive correlation between eruptive volume and repose period in all of the six cases considered and are consistent with the null hypothesis that repose times and eruption volumes are unrelated. There is thus no evidence of time-predictable or volume-predictable behavior for the historical Canary Island volcanism. The rough mean eruption recurrence interval of 39 ± 24 years, while imprecise, may thus be our best current guide for decadal–centurial eruption forecasting in the Canaries.

6. Implications for hazard assessment

Despite infrequent unrest and decadal–millennial repose periods between eruptions, volcanic hazards and risk are far from trivial in the Canary Islands. Indeed, small insular territories tend to be particularly vulnerable to volcanic hazards because large proportions of their population may be exposed. In the Canaries, the entirety of the population lives within a 100 km radius of a Holocene volcano, and as a result the archipelago ranks in the top 20 (13th) countries or territories in terms of proportional volcanic threat (Brown et al., 2015a, 2015b). Table 3 lists Canary Island volcanoes in terms of the Volcanic Hazard Index (VHI) (Auker et al., 2015) and the Population Exposure Index (PEI) (Brown et al., 2015b). While La Palma and Tenerife obtain a VHI Level II score (out of a I–III scale), Lanzarote, El Hierro, Gran Canaria, and Fuerteventura do not meet the data requirement of the classification method and are termed 'unclassified' (Brown et al., 2015a). La Gomera, which lacks Quaternary eruptive activity (Paris et al., 2005), is not listed. On a scale of 1–7, Canary Island volcanoes are assigned moderated to high PEI levels of 4 and 5. The combination of the VHI and PEI gives Risk Level II for La Palma and Tenerife.

A sizable body of work on volcanic hazard assessment in the Canary Islands is already available, and it has grown particularly rapidly since the 2011–2012 El Hierro eruption. Studies have focused on (1) the geologic and eruptive history of volcanoes (e.g., Carracedo et al., 2001, 2007; Rodriguez-Gonzalez et al., 2009), (2) the reconstruction of historical eruptions (e.g., Carracedo et al., 1992, 1996; Klügel et al., 1999; Romero Ruiz, 1990; Solana and Aparicio, 1999; Solana, 2012), (3) the identification of hazards and generation of hazard maps (Araña et al., 2000; Becerril et al., 2014; Carracedo et al., 2004; Felpeto et al., 2001; Marrero et al., 2019), (4) the spatial and temporal probability distribution of future eruptions (Becerril et al., 2013, 2014, 2017; Martí and Felpeto, 2010; Sobradelo et al., 2011), and (5) short-term hazard assessment and volcanic crisis management (Bartolini et al., 2014, 2018; García et al., 2014; Marrero et al., 2015; Solana et al., 2017).

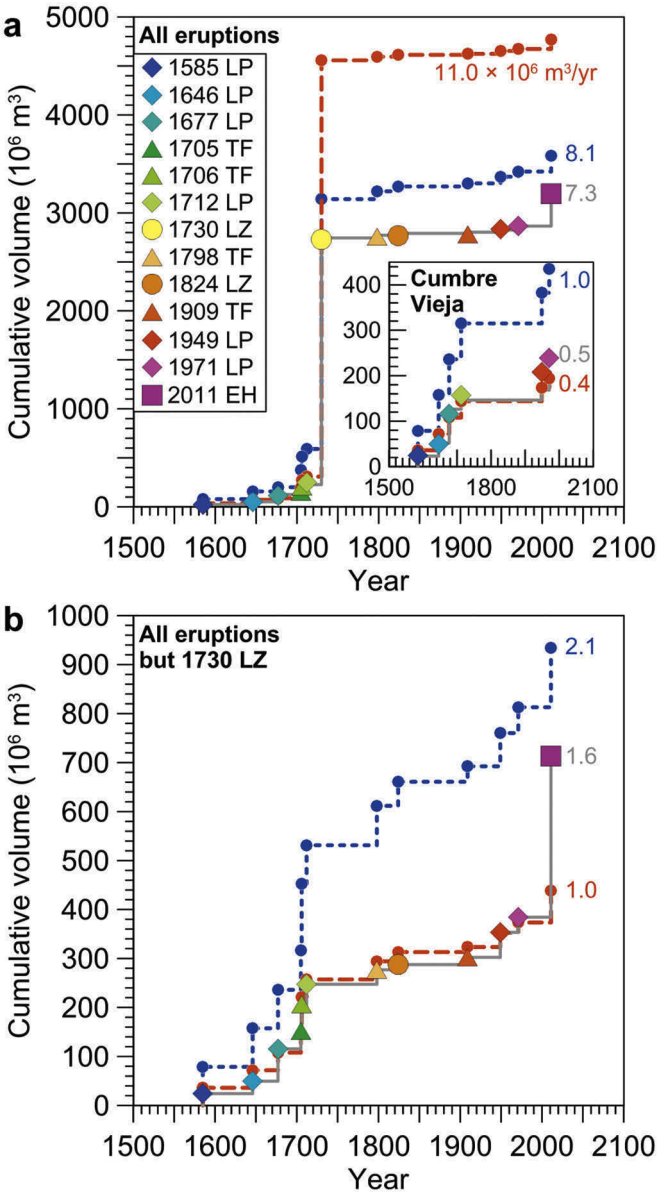

Fig. 11. Cumulative volume curves and eruptive rates. Cumulative volume estimates are plotted against time for (a) all historical eruptions and (b) all eruptions but the 1730–1736 eruption. The inset in (a) shows data for Cumbre Vieja volcano only. In all plots the gray curve with rainbow-colored symbols is constructed using mean field-based volume estimates (Table 1), whereas the navy blue and red curves use the volumes calculated with Eqs. 1 and 2, respectively (Table 2). Colour-coded numbers indicate corresponding mean eruptive rates in 10^6 m^3/year.

The contribution of this paper to improved hazard assessment focuses on categories (2) and, to a lesser extent, (3) above. Our data compilation permits an improved identification and quantification of the eruptive behavior of Canary Island volcanoes in the past 500 years. Excluding the 1730–1736 Timanfaya eruption as an outlier, the following generalizations can be highlighted: (I) Historical records, while incomplete and imprecise, indicate that precursory unrest may begin days to years before eruption onset (see also Albert et al., 2016). For the 2011–2012 event, the only one for which volcano monitoring data are available, unrest began 3 months before the start of the eruption (e.g., López et al., 2012). (II) Eruptions lasted from ten days to a little under five months. (III) Initial eruptive phases usually involved the opening of multiple vents along dike-fed fissures, with Strombolian explosive activity typically focusing at dominant vents situated at

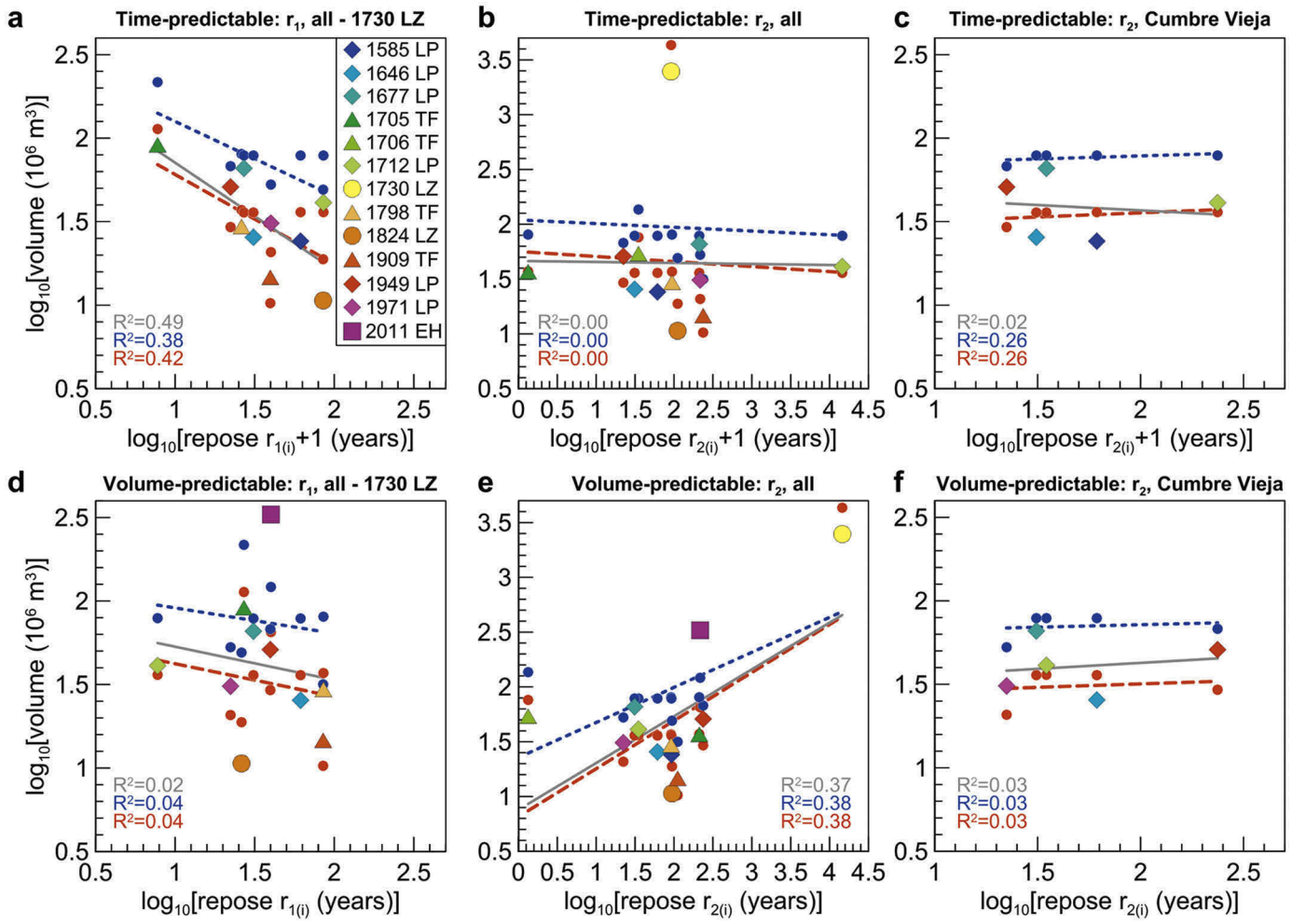

Fig. 12. Tests for time-predictable and volume-predictable behavior of historical eruptions. Following the method of Sandri et al. (2005), the logarithm of eruption volume is plotted against the logarithm of interonset time (referred to as repose period) for different scenarios. Time-predictable scenarios (expected positive correlation of eruption volume and subsequent repose, $r_i + 1$) are shown in (a) using r_1 values (Table 1) for all but the 1730–1736 eruption and treating the 1704–1705 and 1706 eruptions as a single event, (b) using r_2 values (Table 1) for all eruptions and (c) using r_2 values for Cumbre Vieja volcano only. Panels (d), (e) and (f) are the same as (a), (b), and (c), respectively, but for volume-predictable scenarios, whereby a positive correlation between eruption volume and the preceding repose period (r_i) would be expected. In all plots the gray line is the linear regression line for mean published volume estimates (rainbow-colored symbols), whereas the navy blue and red lines are the regression lines for volumes calculated with Eqs. 1 (navy circles) and 2 (red circles), respectively. Corresponding colour-coded coefficients of determination (R^2) are listed. None of the scenarios considered show a significant positive correlation between eruption volume and repose period (see details in Tables A.16–A.17).

higher elevations. Lava effusion generally quickly followed eruption onset. Later eruptive phases were generally characterized by stabilization of the activity dominated by effusive behavior. Some eruptions (1704–1705, 1824, and 1949), however, had a complex evolution punctuated by the opening of distinct vents several kilometers apart. (IV) The main hazards associated with the dominant Strombolian to violent Strombolian eruption style were tephra fall and lava flows. However, hazards associated with volcano-tectonic seismicity and lava dome (1585) and phreatomagmatic (e.g., 1949) eruptive styles also occurred. (V) Total lengths of vent-defined (sometimes discontinuous) fissures range from 0.2 to 14.0 km. (VI) Eruption column height is overall poorly constrained, but lava fountaining heights of up to 700 m have been estimated for the 1909 eruption and other events involved more explosive phreatomagmatic pulses with column height estimates of 1–2 km. (VII) Lava flows reached maximum lengths of 2.7–9.4 km, extending to the coastline in three quarters of eruptions. (VIII) Proximal deposits including vents and associated lava flows covered 1.8–7.8 km^2 and had volumes of 10–330 million m^3. This synthesis provides an important — though clearly not restrictive or exclusive — framework for forecasting the onset, development and style of future Canary Island eruptions.

Nevertheless, many gaps in knowledge remain, and several eruptions are poorly documented. For example, the duration of precursory unrest, which is a particularly useful metric for eruption forecasting efforts, is only very loosely constrained by the historical records. However, petrology-based approaches (e.g., Albert et al., 2015; Longpré et al., 2014) have the potential to quantify volcano reactivation mechanisms and timescales post hoc and should be expanded. In addition, there is a need to further constrain eruption style and magnitude through detailed field-based case studies, especially of tephra fall deposits (e.g., Di Roberto et al., 2016). As a final note, multi-vent eruptions such as those of 1704–1705 (probably also including 1706), 1824 and 1949 and pre-, *syn*-, and post-eruptive seismicity associated with the 2011–2012 eruption (Benito-Saz et al., 2019; Klügel et al., 2015) indicate that magma may migrate over lateral distances reaching at least 20 km before, during and after eruptive phases. The difficulty in forecasting the location of new monogenetic vents during precursory unrest is a significant hurdle in volcanic crisis management in the Canary Islands and other similar localities and calls for a densification of monitoring networks to track magma propagation underground.

Table 3
Classification of Canary Island volcanoes based on the Volcanic Hazard Index and Population Exposure Index, after Brown et al. (2015a)

			Population Exposure Index						
			1	2	3	4	5	6	7
Volcanic Hazard Index	Classified	Hazard III							
		Hazard II				LP; TF			
		Hazard I							
	Unclassified	U-HHR[a]				EH	LZ		
		U-HR[b]				GC			
		U-NHHR[c]				FV			

EH = El Hierro; FV=Fuerteventura; GC = Gran Canaria; LP = La Palma; LZ = Lanzarote; TF = Tenerife.
Yellow = Risk Level I; Orange = Risk Level II; Red = Risk Level III.
[a] Unclassified, with historic and Holocene record.
[b] Unclassified, with Holocene record.
[c] Unclassified, no historic or Holocene record.

7. Conclusions

In this paper, we compile available data on the 13 volcanic eruptions that have taken place in the Canary Islands since 1500 CE, with a focus on their physical characteristics and chronological development. We also report new estimates of key eruption parameters, such as lava flow length, area and volume, and develop a new empirical relationship that may be useful to estimate the volume of basaltic lava flows from their areal extents, in cases where other data are scarce. Our synthesis presents an improved picture of the eruptive behavior of Canary Island volcanoes in the historical period and provides an important framework for forecasting the onset, development and style of future eruptions. The results also allow quantification of the low, modern eruptive rates, which compare surprisingly well with long-term volcano growth rates based on geologic data. The historical eruptive sequence does not display time-predictable or volume-predictable behavior, however. Further work, particularly detailed field-based studies of eruption deposits and petrologic reconstructions of eruption run-up processes, will help refine our understanding of historical volcanism and associated hazards in the Canary Islands.

Supplementary data to this article can be found online at https://doi.org/10.1016/j.jvolgeores.2021.107363.

Declaration of Competing Interest

The authors declare that they have no known competing financial interests or personal relationships that could have appeared to influence the work reported in this paper.

Acknowledgements

We thank Juan Carlos Carracedo and Joan Martí for their help in locating certain sources and pieces of information. The Observatoire Volcanologique du Piton de la Fournaise provided access to the eruption volume dataset of Derrien (2019). M.-A.L. thanks Patrick Beaudry, Lisa Hlinka, James Muller, Samantha Tramontano and John Zayac for fruitful discussions over the course of this project. Reviews by Matthew Patrick and an anonymous referee helped improve this paper. We also thank José Luis Macías for editorial handling. This work is supported through NSF Award #1944723 to M.-A.L.

References

Afonso, A., Aparicio, A., Hernández-Pacheco, A., Rodríguez-Badiola, E., 1974. Morphology evolution of Teneguía volcano area. Estudios Geológicos Teneguía 19–26.

Albert, H., Costa, F., Martí, J., 2015. Timing of magmatic processes and unrest associated with mafic historical monogenetic eruptions in Tenerife Island. J. Petrol. 56, 1945–1966. https://doi.org/10.1093/petrology/egv058.

Albert, H., Costa, F., Martí, J., 2016. Years to weeks of seismic unrest and magmatic intrusions precede monogenetic eruptions. Geology 44, 211–214. https://doi.org/10.1130/G37239.1.

Amelung, F., Day, S.J., 2002. InSAR observations of the 1995 Fogo, Cape Verde, eruption – Implications for the effects of collapse events upon island volcanoes. Geophys. Res. Lett. 29. https://doi.org/10.1029/2001GL013760 , 47-1–47-4..

Araña, V., Felpeto, A., Astiz, M., Garcia, A., Ortiz, R., Abella, R., 2000. Zonation of the main volcanic hazards (lava flows and ash fall) in Tenerife, Canary Islands. A proposal for a surveillance network. J. Volcanol. Geotherm. Res. 103, 377–391. https://doi.org/10.1016/S0377-0273(00)00232-8.

Araña, V., Fuster, J.M., 1974. La erupción del volcán Teneguía, La Palma, Islas Canarias. Estudios Geológicos Teneguía 15–18.

Auker, M.R., Sparks, R.S.J., Jenkins, S.F., Aspinall, W., Brown, S.K., Deligne, N.I., Jolly, G., Loughlin, S.C., Marzocchi, W., Newhall, C.G., Palma, J.L., 2015. Development of a new global Volcanic Hazard Index (VHI). In: Loughlin, S.C., Sparks, R.S.J., Brown, S.K., Jenkins, S.F., Vye-Brown, C. (Eds.), Global Volcanic Hazards and Risk. Cambridge University Press, Cambridge , pp. 349–358. https://doi.org/10.1017/CBO9781316276273.024.

Bagnardi, M., González, P.J., Hooper, A., 2016. High-resolution digital elevation model from tri-stereo Pleiades 1 satellite imagery for lava flow volume estimates at Fogo Volcano. Geophys. Res. Lett. 43, 6267–6275. https://doi.org/10.1002/2016GL069457.

Bartolini, S., Becerril, L., Martí, J., 2014. A new Volcanic managEment Risk Database deslgn (VERDI): application to El Hierro Island (Canary Islands). J. Volcanol. Geotherm. Res. 288, 132–143. https://doi.org/10.1016/j.jvolgeores.2014.10.009.

Bartolini, S., López, C., Becerril, L., Sobradelo, R., Martí, J., 2018. A retrospective study of the pre-eruptive unrest on El Hierro (Canary Islands): implications of seismicity and deformation in the short-term volcanic hazard assessment. Nat. Hazards Earth Syst. Sci. 18, 1759–1770. https://doi.org/10.5194/nhess-18-1759-2018.

Bebbington, M.S., Jenkins, S.F., 2019. Intra-eruption forecasting. Bull. Volcanol. 81, 34. https://doi.org/10.1007/s00445-019-1294-9.

Becerril, L., Cappello, A., Galindo, I., Neri, M., Del Negro, C., 2013. Spatial probability distribution of future volcanic eruptions at El Hierro Island (Canary Islands, Spain). J. Volcanol. Geotherm. Res. 257, 21–30. https://doi.org/10.1016/j.jvolgeores.2013.03.005.

Becerril, L., Bartolini, S., Sobradelo, R., Martí, J., Morales, J.M., Galindo, I., 2014. Long-term volcanic hazard assessment on El Hierro (Canary Islands). Nat. Hazards Earth Syst. Sci. 14, 1853–1870. https://doi.org/10.5194/nhess-14-1853-2014.

Becerril, L., Martí, J., Bartolini, S., Geyer, A., 2017. Assessing qualitative long-term volcanic hazards at Lanzarote Island (Canary Islands). Nat. Hazards Earth Syst. Sci. 17, 1145–1157. https://doi.org/10.5194/nhess-17-1145-2017.

Benito-Saz, M.A., Sigmundsson, F., Charco, M., Hooper, A., Parks, M., 2019. Magma flow rates and temporal evolution of the 2012–2014 post-eruptive intrusions at El Hierro, Canary Islands. J. Geophys. Res. Solid Earth 124, 12576–12592. https://doi.org/10.1029/2019JB018219.

Bonelli Rubio, J.M., 1950. Contribución al Estudio de la Erupción del Volcán del Nambroque o San Juan (Isla de La Palma) 24 de Junio – 4 de Agosto de 1949, Talleres del Instituto Geográfico y Catastral. Instituto Geográfico y Catastral, Madrid, pp. 1–22.

Brown, S.K., Sparks, R.S.J., Mee, K., Vye-Brown, C., Ilyinskaya, E., Jenkins, S.F., Loughlin, S.C., 2015a. Country and regional profiles of volcanic hazard and risk. In: Loughlin, S.C., Sparks, R.S.J., Brown, S.K., Jenkins, S.F., Vye-Brown, C. (Eds.), Global Volcanic Hazards and Risk. Cambridge University Press, Cambridge.

Brown, S.K., Auker, M.R., Sparks, R.S.J., 2015b. Populations around Holocene volcanoes and development of a Population Exposure Index. In: Loughlin, S.C., Sparks, R.S.J., Brown, S.K., Jenkins, S.F., Vye-Brown, C. (Eds.), Global Volcanic Hazards and Risk. Cambridge University Press, Cambridge, pp. 223–232 https://doi.org/10.1017/CBO9781316276273.006.

Burt, M., Wadge, G., Scott, W., 1994. Simple stochastic modelling of the eruption history of a basaltic volcano: Nyamuragira, Zaire. Bull. Volcanol. 56, 87–97. https://doi.org/10.1007/BF00304104.
Carracedo, J.C., 2013. The last 2 ky of eruptive activity on the Teide Volcanic Complex: Features and trends. In: Carracedo, J.C., Troll, V.R. (Eds.), Teide Volcano. Springer-Verlag, Berlin, Heidelberg , pp. 129–153. https://doi.org/10.1007/978-3-642-25893-0_8.
Carracedo, J., 2014. The 1730–1736 Eruption of Lanzarote, Canary Islands. In: Gutiérrez, F., Gutiérrez, M. (Eds.), Landscapes and Landforms of Spain, World Geomorphological Landscapes. Springer Netherlands, pp. 273–288 https://doi.org/10.1007/978-94-017-8628-7_23.
Carracedo, J.C., Rodríguez Badiola, E., 1991. Lanzarote. La erupción volcánica de 1730. Cabildo Insular de Lanzarote. Servicios de Publicaciones, Las Palmas de Gran Canaria.
Carracedo, J.C., Troll, V.R., 2016. The Geology of the Canary Islands. 1st ed. Elsevier https://doi.org/10.1016/C2015-0-04268-X.
Carracedo, J.C., Rodríguez Badiola, E., Soler, V., 1990. Aspectos volcanológicos y estructurales, evolución petrológica e implicaciones en riesgo volcánico de la erupción de 1730 en Lanzarote, Islas Canarias. Estud. Geol. 46, 25–55.
Carracedo, J.C., Rodríguez Badiola, E., Soler, V., 1992. The 1730-1736 eruption of Lanzarote, Canary Islands: a long, high-magnitude basaltic fissure eruption. J. Volcanol. Geotherm. Res. 53, 239–250. https://doi.org/10.1016/0377-0273(92)90084-Q.
Carracedo, J.C., Day, S., Guillou, H., Rodríguez Badiola, E., 1996. The 1677 eruption of La Palma, Canary Islands. Estud. Geol. 52, 103–114. https://doi.org/10.3989/egeol.96523-4258.
Carracedo, J.C., Day, S.J., Guillou, H., Rodríguez Badiola, E., Canas, J.A., Pérez Torrado, F.J., 1998. Hotspot volcanism close to a passive continental margin: the Canary Islands. Geol. Mag. 135, 591–604. https://doi.org/10.1017/S0016756898001447.
Carracedo, J.C., Day, S.J., Guillou, H., Gravestock, P., 1999a. Later stages of volcanic evolution of La Palma, Canary Islands; rift evolution, giant landslides, and the genesis of the Caldera de Taburiente. Geol. Soc. Am. Bull. 111, 755–768.
Carracedo, Juan Carlos, Day, S.J., Guillou, H., Pérez Torrado, F.J., 1999b. Giant Quaternary landslides in the evolution of La Palma and El Hierro, Canary Islands. J. Volcanol. Geotherm. Res. 94, 169–190.
Carracedo, J.C., Rodríguez Badiola, E., Guillou, H., de la Nuez, J., Pérez Torrado, F.J., 2001. Geology and volcanology of La Palma and El Hierro, Western Canaries. Estud. Geol. 57, 175–273.
Carracedo, J.C., Singer, B., Jicha, B., Guillou, H., Rodríguez Badiola, E., Meco, J., Pérez Torrado, F.J., Gimeno, D., Socorro, J.S., Láinez, A., 2003. La erupción y el tubo volcánico del volcán Corona (Lanzarote, Islas Canarias). Estud. Geol. 59, 277–302.
Carracedo, J.C., Guillou, H., Paterne, M., Scaillet, S., Rodríguez Badiola, E., Paris, R., Pérez Torrado, F.J., Hansen Machín, A., 2004. Análisis del riesgo volcánico asociado al flujo de lavas en Tenerife (Islas Canarias): escenarios previsibles para una futura erupción en la isla. Estud. Geol. 60, 63–93. https://doi.org/10.3989/egeol.04603-675.
Carracedo, J.C., Rodríguez Badiola, E., Guillou, H., Paterne, M., Scaillet, S., Pérez Torrado, F.J., Paris, R., Fra-Paleo, U., Hansen, A., 2007. Eruptive and structural history of Teide Volcano and rift zones of Tenerife, Canary Islands. Geol. Soc. Am. Bull. 119, 1027–1051. https://doi.org/10.1130/b26087.1.
Carracedo, J.C., Rodriguez-Gonzalez, A., Pérez-Torrado, F.J., Fernandez-Turiel, J.-L., Paris, R., Rodríguez-Badiola, E., Pestana-Pérez, G., Troll, V.R., Wiesmaier, S., 2013. Geological hazards in the Teide Volcanic Complex. In: Carracedo, J.C., Troll, V.R. (Eds.), Teide Volcano. Springer-Verlag, Berlin, Heidelberg , pp. 249–272. https://doi.org/10.1007/978-3-642-25893-0_8.
Carracedo, J.C., Troll, V.R., Zaczek, K., Rodríguez-González, A., Soler, V., Deegan, F.M., 2015. The 2011–2012 submarine eruption off El Hierro, Canary Islands: new lessons in oceanic island growth and volcanic crisis management. Earth Sci. Rev. 150, 168–200. https://doi.org/10.1016/j.earscirev.2015.06.007.
Dávila y Cárdenas, P.M., 1737. Constituciones y Nuevas Addiciones Synodales del Obispado de las Canarias Madrid.
Day, S.J., Carracedo, J.C., Guillou, H., Gravestock, P., 1999. Recent structural evolution of the Cumbre Vieja volcano, La Palma, Canary Islands: volcanic rift zone reconfiguration as a precursor to volcano flank instability? J. Volcanol. Geotherm. Res. 94, 135–167. https://doi.org/10.1016/S0377-0273(99)00101-8.
De la Cruz-Reyna, S., 1993. Random patterns of occurrence of explosive eruptions at Colima Volcano, Mexico. J. Volcanol. Geotherm. Res. 55, 51–68. https://doi.org/10.1016/0377-0273(93)90089-A.
Derrien, A., 2019. Apport des Techniques Photogrammétriques à L'étude du Dynamisme des Structures Volcaniques du Piton de la Fournaise. Institut de Physique du Globe de Paris. Université Sorbonne Paris Cité.
Di Roberto, A., Bertagnini, A., Del Carlo, P., Meletlidis, S., Pompilio, M., 2016. The 1909 Chinyero eruption on Tenerife (Canary Islands): insights from historical accounts, and tephrostratigraphic and geochemical data. Bull. Volcanol. 78, 88. https://doi.org/10.1007/s00445-016-1083-7.
Domínguez Cerdeña, I., García-Cañada, L., Benito-Saz, M.A., del Fresno, C., Lamolda, H., Pereda de Pablo, J., Sánchez Sanz, C., 2018. On the relation between ground surface deformation and seismicity during the 2012–2014 successive magmatic intrusions at El Hierro Island. Tectonophysics 744, 422–437. https://doi.org/10.1016/j.tecto.2018.07.019.
Dvorak, J.J., Dzurisin, D., 1993. Variations in magma supply rate at Kilauea volcano, Hawaii. J. Geophys. Res. 98, 22255–22268. https://doi.org/10.1029/93JB02765.
Felpeto, A., Araña, V., Ortiz, R., Astiz, M., García, A., 2001. Assessment and modelling of lava flow hazard on Lanzarote (Canary Islands). Nat. Hazards 23, 247–257. https://doi.org/10.1023/A:1011112330766.
Fernández Navarro, L., 1911. Erupción volcánica del Chinyero (Tenerife) en noviembre de 1909. Anales de la Junta para Ampliación de Estudios e Investigaciones Científicas, V, Mem. 1, p. 99.
Fernández Santín, S., Hernán Reguera, F., Navarro Falcones, L.F., Pliego Dones, D., 1974. Petrographic study of basaltic materials emitted by Teneguía volcano (La Palma, Canary Islands, October 27th–November 19th, 1971). Estudios Geológicos Teneguía 27–33.
French, S.W., Romanowicz, B., 2015. Broad plumes rooted at the base of the Earth's mantle beneath major hotspots. Nature 525, 95–99. https://doi.org/10.1038/nature14876.
Fullea, J., Camacho, A.G., Negredo, A.M., Fernández, J., 2015. The Canary Islands hot spot: new insights from 3D coupled geophysical–petrological modelling of the lithosphere and uppermost mantle. Earth Planet. Sci. Lett. 409, 71–88. https://doi.org/10.1016/j.epsl.2014.10.038.
García, A., Berrocoso, M., Marrero, J.M., Fernández-Ros, A., Prates, G., De la Cruz-Reyna, S., Ortiz, R., 2014. Volcanic alert system (VAS) developed during the 2011–2014 El Hierro (Canary Islands) volcanic process. Bull. Volcanol. 76, 825. https://doi.org/10.1007/s00445-014-0825-7.
Geldmacher, J., Hoernle, K., Bogaard, P.V.D., Duggen, S., Werner, R., 2005. New $^{40}Ar/^{39}Ar$ age and geochemical data from seamounts in the Canary and Madeira volcanic provinces: support for the mantle plume hypothesis. Earth Planet. Sci. Lett. 237, 85–101. https://doi.org/10.1016/j.epsl.2005.04.037.
González, P.J., Samsonov, S.V., Pepe, S., Tiampo, K.F., Tizzani, P., Casu, F., Fernández, J., Camacho, A.G., Sansosti, E., 2013. Magma storage and migration associated with the 2011–2012 El Hierro eruption: Implications for crustal magmatic systems at oceanic island volcanoes. J. Geophys. Res. Solid Earth 118, 4361–4377. https://doi.org/10.1002/jgrb.50289.
Gregg, T.K., Fornari, D.J., 1998. Long submarine lava flows: Observations and results from numerical modeling. J. Geophys. Res. Solid Earth 103, 27517–27531. https://doi.org/10.1029/98JB02465.
Gregg, C.E., Houghton, B.F., Johnston, D.M., Paton, D., Swanson, D.A., 2004. The perception of volcanic risk in Kona communities from Mauna Loa and Hualālai volcanoes, Hawai'i. J. Volcanol. Geotherm. Res. 130, 179–196. https://doi.org/10.1016/S0377-0273(03)00288-9.
Hernandez-Pacheco, A., Valls, M.C., 1982. The historic eruptions of La Palma Island (Canaries). Arquipélago. Série Ciências da Natureza 3, 83–94.
Herzberg, C., Asimow, P.D., 2008. Petrology of some oceanic island basalts: PRIMELT2.XLS software for primary magma calculation. Geochem. Geophys. Geosyst. 9. https://doi.org/10.1029/2008GC002057 Q09001.
Hill, B.E., Connor, C.B., Jarzemba, M.S., La Femina, P.C., Navarro, M., Strauch, W., 1998. 1995 eruptions of Cerro Negro Volcano, Nicaragua, and risk assessment for future eruptions. Bull. Geol. Soc. Am. 110, 1231–1241. https://doi.org/10.1130/0016-7606(1998)110<1231:EOCNVN>2.3.CO;2.
Hoernle, K., Schmincke, H.-U., 1993. The role of partial melting in the 15-Ma geochemical evolution of Gran Canaria: a blob model for the Canary Hotspot. J. Petrol. 34, 599–626. https://doi.org/10.1093/petrology/34.3.599.
Houghton, B.F., Cockshell, W.A., Gregg, C.E., Walker, B.H., Kim, K., Tisdale, C.M., Yamashita, E., 2021. Land, lava, and disaster create a social dilemma after the 2018 eruption of Kīlauea volcano. Nat. Commun. 12, 1223. https://doi.org/10.1038/s41467-021-21455-2.
Instituto Canario de Estadística, 2016. Canarias en Cifras.
Kervyn, M., Ernst, G.G.J., Carracedo, J.C., Jacobs, P., 2012. Geomorphometric variability of "monogenetic" volcanic cones: evidence from Mauna Kea, Lanzarote and experimental cones. Geomorphology 136, 59–75. https://doi.org/10.1016/j.geomorph.2011.04.009.
Kilburn, C.R., 2004. Fracturing as a quantitative indicator of lava flow dynamics. J. Volcanol. Geotherm. Res. 132, 209–224. https://doi.org/10.1016/S0377-0273(03)00346-9.
Kilburn, C.R., 2015. Lava flow hazards and modeling. The Encyclopedia of Volcanoes. Elsevier, pp. 957–969.
Klügel, A., Schmincke, H.-U., White, J.D.L., Hoernle, K.A., 1999. Chronology and volcanology of the 1949 multi-vent rift-zone eruption on La Palma (Canary Islands). J. Volcanol. Geotherm. Res. 94, 267–282. https://doi.org/10.1016/S0377-0273(99)00107-9.
Klügel, A., Longpré, M.-A., García-Cañada, L., Stix, J., 2015. Deep intrusions, lateral magma transport and related uplift at ocean island volcanoes. Earth Planet. Sci. Lett. 431, 140–149. https://doi.org/10.1016/j.epsl.2015.09.031.
Kueppers, U., Nichols, A., Zanon, V., Potuzak, M., Pacheco, J., 2012. Lava balloons—peculiar products of basaltic submarine eruptions. Bull. Volcanol. 74, 1379–1393. https://doi.org/10.1007/s00445-012-0597-x.
Kueppers, U., Pimentel, A., Ellis, B., Forni, F., Neukampf, J., Pacheco, J., Perugini, D., Queiroz, G., 2019. Biased volcanic hazard assessment due to incomplete eruption records on Ocean Islands: an Example of Sete Cidades Volcano, Azores. Front. Earth Sci. 7. https://doi.org/10.3389/feart.2019.00122.
Longpré, M.-A., Klügel, A., Diehl, A., Stix, J., 2014. Mixing in mantle magma reservoirs prior to and during the 2011–2012 eruption at El Hierro, Canary Islands. Geology 42, 315–318. https://doi.org/10.1130/g35165.1.
Longpré, M.-A., Stix, J., Klügel, A., Shimizu, N., 2017. Mantle to surface degassing of carbon- and sulphur-rich alkaline magma at El Hierro, Canary Islands. Earth Planet. Sci. Lett. 460, 268–280. https://doi.org/10.1016/j.epsl.2016.11.043.
López, C., Blanco, M.J., Abella, R., Brenes, B., Cabrera Rodríguez, V.M., Casas, B., Domínguez Cerdeña, I., Felpeto, A., de Villalta, M.F., del Fresno, C., García, O., García-Arias, M.J., García-Cañada, L., Gomis Moreno, A., González-Alonso, E., Guzmán Pérez, J., Iribarren, I., López-Díaz, R., Luengo-Oroz, N., Meletlidis, S., Moreno, M., Moure, D., de Pablo, J.P., Rodero, C., Romero, E., Sainz-Maza, S., Sentre Domingo, M.A., Torres, P.A., Trigo, P., Villasante-Marcos, V., 2012. Monitoring the volcanic unrest of El Hierro (Canary Islands) before the onset of the 2011-2012 submarine eruption. Geophys. Res. Lett. 39, L13303. https://doi.org/10.1029/2012gl051846.
Marrero, J.M., García, A., Llinares, Á., Berrocoso, M., Ortiz, R., 2015. Legal framework and scientific responsibilities during volcanic crises: the case of the El Hierro eruption (2011–2014). J. Appl. Volcanol. 4, 13. https://doi.org/10.1186/s13617-015-0028-8.

Marrero, J.M., García, A., Berrocoso, M., Llinares, Á., Rodríguez-Losada, A., Ortiz, R., 2019. Strategies for the development of volcanic hazard maps in monogenetic volcanic fields: the example of La Palma (Canary Islands). J. Appl. Volcanol. 8, 6. https://doi.org/10.1186/s13617-019-0085-5.

Martí, J., Felpeto, A., 2010. Methodology for the computation of volcanic susceptibility: An example for mafic and felsic eruptions on Tenerife (Canary Islands). J. Volcanol. Geotherm. Res. 195, 69–77. https://doi.org/10.1016/j.jvolgeores.2010.06.008.

Martí, J., Pinel, V., López, C., Geyer, A., Abella, R., Tárraga, M., Blanco, M.J., Castro, A., Rodríguez, C., 2013a. Causes and mechanisms of the 2011–2012 El Hierro (Canary Islands) submarine eruption. J. Geophys. Res. Solid Earth 118. https://doi.org/10.1002/jgrb.50087.

Martí, J., Castro, A., Rodríguez, C., Costa, F., Carrasquilla, S., Pedreira, R., Bolos, X., 2013b. Correlation of magma evolution and geophysical monitoring during the 2011–2012 El Hierro (Canary Islands) submarine eruption. J. Petrol. 54, 1349–1373. https://doi.org/10.1093/petrology/egt014.

Marzocchi, W., Bebbington, M.S., 2012. Probabilistic eruption forecasting at short and long time scales. Bull. Volcanol. 74, 1777–1805. https://doi.org/10.1007/s00445-012-0633-x.

Meletlidis, S., Di Roberto, A., Cerdeña, I.D., Pompilio, M., Bertagnini, A., Benito-Saz, M.A., Del Carlo, P., Aparicio, S.S.-M., 2015. New insight into the 2011-2012 unrest and eruption of El Hierro Island (Canary Islands) based on integrated geophysical, geodetical and petrological data. Ann. Geophys. 58, S0546. https://doi.org/10.4401/ag-6754.

Michon, L., Staudacher, T., Ferrazzini, V., Bachèlery, P., Martí, J., 2007. April 2007 collapse of Piton de la Fournaise: A new example of caldera formation. Geophys. Res. Lett. 34, L21301. https://doi.org/10.1029/2007GL031248.

Muller, J.K., 2016. Tephrostratigraphy of the AD 1730–1736 Timanfaya Eruption, Lanzarote, Canary Islands: Insights into the Dynamics of Large Basaltic Fissure Eruptions. Queens College, City University of New York.

Murray, J., Stevens, N., 2000. New formulae for estimating lava flow volumes at Mt. Etna Volcano, Sicily. Bull. Volcanol. 61, 515–526. https://doi.org/10.1007/s004450050002.

Neal, C.A., Brantley, S.R., Antolik, L., Babb, J.L., Burgess, M., Calles, K., Cappos, M., Chang, J.C., Conway, S., Desmither, L., Dotray, P., Elias, T., Fukunaga, P., Fuke, S., Johanson, I.A., Kamibayashi, K., Kauahikaua, J., Lee, R.L., Pekalib, S., Miklius, A., Million, W., Moniz, C.J., Nadeau, P.A., Okubo, P., Parcheta, C., Patrick, M.R., Shiro, B., Swanson, D.A., Tollett, W., Trusdell, F., Younger, E.F., Zoeller, M.H., Montgomery-Brown, E.K., Anderson, K.R., Poland, M.P., Ball, J.L., Bard, J., Coombs, M., Dietterich, H.R., Kern, C., Thelen, W.A., Cervelli, P.F., Orr, T., Houghton, B.F., Gansecki, C., Hazlett, R., Lundgren, P., Diefenbach, A.K., Lerner, A.H., Waite, G., Kelly, P., Clor, L., Werner, C., Mulliken, K., Fisher, G., Damby, D., 2019. The 2018 rift eruption and summit collapse of Kīlauea Volcano. Science 363, 367–374. https://doi.org/10.1126/science.aav7046.

Ortiz, R., Araña, V., Valverde, C., 1986. Aproximación al conocimiento del mecanismo de la erupción de 1730-1736 en Lanzarote. Anales de Física 82, 127–142.

Pallarés Padilla, A., 2007. Nuevas aportaciones al conocimiento de la erupción de Timanfaya (Lanzarote). Académico de Número, Academia de Ciencias e Ingenierías de Lanzarote 45.

Paris, R., Guillou, H., Carracedo, J.C., Pérez Torrado, F.J., 2005. Volcanic and morphological evolution of La Gomera (Canary Islands), based on new K-Ar ages and magnetic stratigraphy: implications for oceanic island evolution. J. Geol. Soc. Lond. 162, 501–512. https://doi.org/10.1144/0016-764904-055.

Pedersen, G.B.M., Höskuldsson, A., Dürig, T., Thordarson, T., Jonsdottir, I., Riishuus, M.S., Óskarsson, B.V., Dumont, S., Magnússon, E., Gudmundsson, M.T., 2017. Lava field evolution and emplacement dynamics of the 2014–2015 basaltic fissure eruption at Holuhraun, Iceland. J. Volcanol. Geotherm. Res. 340, 155–169. https://doi.org/10.1016/j.jvolgeores.2017.02.027.

Ponte y Cologán, A., 1911. Volcán del Chinyero. Memoria Histórico- Descriptiva de Esta Erupción Volcánica Acaecida en 18 de Noviembre de 1909 Tipolit, Tenerife.

Pyle, D.M., 2015. Sizes of volcanic eruptions. The Encyclopedia of Volcanoes. Elsevier, pp. 257–264.

Real Audiencia de Canarias, 1731. Copia de las Ordenes, y providencias dadas para el alivio de los Vezinos de la Isla de Lanzarotte en su dilatado padezer a causa del prodigioso Volcan, queen ella rebentó el primer dia de Septiembre del afio immediato pasado de 1730, y continúa asta el dia de la fecha. Va inserto el Mapa de la Isla, del Volcan, y sus bocas con la descripcion del miserable estado aque tiene reducida la Isla. Canaria y Abril 4 de 1731. Legajo Manuscrito de la Real Audiencia de Canarias, Gracia y Justicia, Leg, p. 89.

Rivera, J., Lastras, G., Canals, M., Acosta, J., Arrese, B., Hermida, N., Micallef, A., Tello, O., Amblas, D., 2013. Construction of an oceanic island: Insights from the El Hierro (Canary Islands) 2011–2012 submarine volcanic eruption. Geology 41, 355–358. https://doi.org/10.1130/g33863.1.

Rivera, J., Hermida, N., Arrese, B., González-Aller, D., Sánchez de Lamadrid, J.L., Gutiérrez de la Flor, D., Acosta, J., 2014. Bathymetry of a new-born submarine volcano: El Hierro. Canary Islands. J. Maps 10, 82–89. https://doi.org/10.1080/17445647.2013.849620.

Rodriguez-Gonzalez, A., Fernandez-Turiel, J.L., Perez-Torrado, F.J., Hansen, A., Aulinas, M., Carracedo, J.C., Gimeno, D., Guillou, H., Paris, R., Paterne, M., 2009. The Holocene volcanic history of Gran Canaria island: implications for volcanic hazards. J. Quat. Sci. 24, 697–709. https://doi.org/10.1002/jqs.1294.

Romero, C., 2003. El Relieve de Lanzarote. Servicio de Publicaciones, Cabildo de Lanzarote.

Romero Ortiz, J., 1951. La erupción del Nambroque en la Isla de la Palma. Boletín del Instituto Geológico y Minero de España 63 164 pp.

Romero Ruiz, C., 1990. Las Manifestaciones Volcánicas Históricas del Archipiélago Canario. Universidad de La Laguna.

Romero Ruiz, C., Beltrán Yanes, E., 2015. El impacto de las coladas de 1706 en la ciudad de Garachico. (Tenerife, Islas Canarias, España). Investigaciones Geográficas 63, 99–115. https://doi.org/10.14198/INGEO2015.63.07.

Rueda Núñez, J.J., Abella Meléndez, R., Blanco Sánchez, M.J., Díaz Suárez, E.A., Domínguez Cerdeña, I.F., Domínguez Valbuena, J., Fernández de Villalta Compagni, M., del Fresno Rodríguez-Portugal, C., López Díaz, R., López Moreno, C., López Muga, M., Muñoz Santamaría, A., Sánchez Sanz, C., Mezcua Rodríguez, J., 2020. Revisión del catálogo sísmico de las Islas Canarias (1341-2000). Administración General del Estado, Madrid, 1st ed. https://doi.org/10.7419/162.34.2020.

Sánchez, C., 2014. Revisión del catálogo sísmico de las Islas Canarias. Universidad Politécnica de Madrid, Madrid.

Sánchez-Pastor, P., Obermann, A., Schimmel, M., 2018. Detecting and locating precursory signals during the 2011 El Hierro, Canary Islands, submarine eruption. Geophys. Res. Lett. 45, 10,288–10,297. https://doi.org/10.1029/2018gl079550.

Sandri, L., Marzocchi, W., Gasperini, P., 2005. Some insights on the occurrence of recent volcanic eruptions of Mount Etna volcano (Sicily, Italy). Geophys. J. Int. 163, 1203–1218. https://doi.org/10.1111/j.1365-246X.2005.02757.x.

Sobradelo, R., Martí, J., Mendoza-Rosas, A.T., Gómez, G., 2011. Volcanic hazard assessment for the Canary Islands (Spain) using extreme value theory. Nat. Hazards Earth Syst. Sci. 11, 2741–2753. https://doi.org/10.5194/nhess-11-2741-2011.

Solana, M.C., 2012. Development of unconfined historic lava flow fields in Tenerife: implications for the mitigation of risk from a future eruption. Bull. Volcanol. 74, 2397–2413. https://doi.org/10.1007/s00445-012-0670-5.

Solana, M., Aparicio, A., 1999. Reconstruction of the 1706 Montaña Negra eruption. Emergency procedures for Garachico and El Tanque, Tenerife, Canary Islands. Geol. Soc. Lond., Spec. Publ. 161, 209–216. https://doi.org/10.1144/GSL.SP.1999.161.01.14.

Solana, M.C., Kilburn, C.R.J., Rodríguez Badiola, E., Aparicio, A., 2004. Fast emplacement of extensive pahoehoe flow-fields: the case of the 1736 flows from Montana de las Nueces, Lanzarote. J. Volcanol. Geotherm. Res. 132, 189–207. https://doi.org/10.1016/S0377-0273(03)00345-7.

Solana, M., Calvari, S., Kilburn, C., Gutierrez, H., Chester, D., Duncan, A., 2017. Supporting the development of procedures for communications during volcanic emergencies: Lessons learnt from the Canary Islands (Spain) and Etna and Stromboli (Italy). In: Fearnley, C.J., Bird, D.K., Haynes, K., McGuire, W.J., Jolly, G. (Eds.), Observing the Volcano World. Advances in Volcanology. Springer , pp. 289–305. https://doi.org/10.1007/11157_2016_48.

Somoza, L., González, F., Barker, S., Madureira, P., Medialdea, T., de Ignacio, C., Lourenço, N., León, R., Vázquez, J., Palomino, D., 2017. Evolution of submarine eruptive activity during the 2011-2012 El Hierro event as documented by hydroacoustic images and remotely operated vehicle observations. Geochem. Geophys. Geosyst. 18, 3109–3137. https://doi.org/10.1002/2016GC006733.

Sparks, R.S.J., 2003. Forecasting volcanic eruptions. Earth Planet. Sci. Lett. 210, 1–15. https://doi.org/10.1016/S0012-821X(03)00124-9.

Tarquini, S., Favalli, M., 2011. Mapping and DOWNFLOW simulation of recent lava flow fields at Mount Etna. J. Volcanol. Geotherm. Res. 204, 27–39. https://doi.org/10.1016/j.jvolgeores.2011.05.001.

Thordarson, T., Self, S., 1993. The Laki (Skaftár Fires) and Grímsvötn eruptions in 1783–1785. Bull. Volcanol. 55, 233–263. https://doi.org/10.1007/BF00624353.

Troll, V.R., Klügel, A., Longpré, M.-A., Burchardt, S., Deegan, F.M., Carracedo, J.C., Wiesmaier, S., Kueppers, U., Dahren, B., Blythe, L.S., Hansteen, T.H., Freda, C., Budd, D.A., Jolis, E.M., Jonsson, E., Meade, F.C., Harris, C., Berg, S.E., Mancini, L., Polacci, M., Pedroza, K., 2012. Floating stones off El Hierro, Canary Islands: xenoliths of preisland sedimentary origin in the early products of the October 2011 eruption. Solid Earth 3, 97–110. https://doi.org/10.5194/se-3-97-2012.

van den Bogaard, P., 2013. The origin of the Canary Island Seamount Province-New ages of old seamounts. Sci. Rep. 3, 2107. https://doi.org/10.1038/srep02107.

Villasante-Marcos, V., Pavón-Carrasco, F.J., 2014. Palaeomagnetic constraints on the age of Lomo Negro volcanic eruption (El Hierro, Canary Islands). Geophys. J. Int. 199, 1497–1514. https://doi.org/10.1093/gji/ggu346.

von Buch, L., 1825. Physikalische Beschreibung der Canarischen Inseln.

Wadge, G., 1982. Steady state volcanism: evidence from eruption histories of polygenetic volcanoes. J. Geophys. Res. Solid Earth 87, 4035–4049. https://doi.org/10.1029/JB087iB05p04035.

White, J.D.L., Schmincke, H.-U., 1999. Phreatomagmatic eruptive and depositional processes during the 1949 eruption on La Palma (Canary Islands). J. Volcanol. Geotherm. Res. 94, 283–304. https://doi.org/10.1016/S0377-0273(99)00108-0.

White, S.M., Crisp, J.A., Spera, F.J., 2006. Long-term volumetric eruption rates and magma budgets. Geochem. Geophys. Geosyst. 7, Q03010. https://doi.org/10.1029/2005GC001002.

Zaczek, K., Troll, V.R., Cachao, M., Ferreira, J., Deegan, F.M., Carracedo, J.C., Soler, V., Meade, F.C., Burchardt, S., 2015. Nannofossils in 2011 El Hierro eruptive products reinstate plume model for Canary Islands. Sci. Rep. 5. https://doi.org/10.1038/srep07945.